



DELFT UNIVERSITY OF TECHNOLOGY

DEPARTMENT OF AEROSPACE ENGINEERING

Report LR-297

**STRESS GRADIENTS AROUND NOTCHES**

**J. Schijve**

DELFT - THE NETHERLANDS

April 1980

ERRATUM Report LR-297

(Stress gradients around notches)

page 3: Eq. (10): 
$$S_{fK} = \frac{S_{f1}}{K_t} \left( 1 + 2 \sqrt{\frac{2}{\rho}} \right) \quad (10)$$

Line 3 under table: ... especially so for sharp notches ...

page 10: Line 3: ... a large conformity ...

page 11: Line above Eq. (18): ... stress gradient expressed in Eq. (11) ..

page 12: Line under Eq. (24): ... appear from  $\beta$  values ..

First line of 7.2: ... and the nominal stress, ...

page 13: Last sentence before 7.3: ... will apply to bending ..

Line 5 of 7.3: ... highly stressed ...

Bottom line: Furthermore, ...



DELFT UNIVERSITY OF TECHNOLOGY

DEPARTMENT OF AEROSPACE ENGINEERING

Report LR-297

**STRESS GRADIENTS AROUND NOTCHES**

**J. Schijve**

DELFT - THE NETHERLANDS

April 1980

## ABSTRACT

Stress gradients at the root of a notch are significant for the notch effect and the size effect on fatigue properties. Usually the gradient of the stress distribution in the minimum section is considered. In the present paper the variation of the tensile stress along the edge of the notch is considered. Calculations are made for a variety of notches. The results indicate a remarkable conformity of stress distributions at the notch root if the same peak stress and notch root radius ( $\rho$ ) apply. Consequently  $K_t$  and  $\rho$  are highly characteristic for the stress distribution around the notch. Along the edge of the notch the stress decreases at a much slower rate than in the minimum section going away from the material surface. For the stress along the edge of the notch a stress gradient coefficient is defined. The variation of this coefficient is fairly small for several notches and  $K_t$  values. A 5 percent lower stress as compared to the peak stress at the notch root is obtained at about  $0.02 \rho$  below the material surface and at a distance of about  $0.18 \rho$  to the critical point along the material surface.

## NOTATIONS

$a$	semi axis of ellips, hole radius
$\alpha$	material constant
$b$	semi axis of ellips
$d_1, d_2$	co-ordinates for a certain decrease of stress (Fig. 3)
$K_t$	theoretical stress concentration factor
$K_f$	fatigue strength reduction factor
$N$	fatigue life
$q$	notch sensitivity factor
$S$	nominal stress
$S_1$	main principal stress
$S_{f1}$	fatigue limit of unnotched material
$S_{fK}$	fatigue limit of notched element
$\alpha$	stress gradient coefficient (Eq. 11)
$\beta$	second stress gradient coefficient (Eq. 23)
$\gamma$	$S_1/\sigma_{\text{peak}}$
$\rho$	notch root radius
$\sigma_{\text{peak}}$	peak stress at notch root
$\chi$	relative stress gradient in minimum section (Eq. 12)

## CONTENTS

- 1 Introduction
- 2 The notch effect and stress gradients
- 3 Notch effect, size effect and different stress gradients
- 4 The stress gradient coefficient  $\alpha$
- 5 The gradient ratio  $d_2/d_1$
- 6 Stress distributions for three different holes
- 7 Discussion
  - 7.1 Evaluation of the calculated results
  - 7.2 Characterisation of the notch severity
  - 7.3  $K_f$ - $K_t$  relations
- 8 Conclusions
- 9 References

Appendix A: The stress gradient coefficient  $\alpha$  and  $K_t$  for hyperbolic notches and an elliptical hole

Appendix B: Stress gradients around circular holes according to the studies of Howland and Schulz

Appendix C: Stress distributions around hyperbolic notches in infinite material

Appendix D: Stress distributions around elliptical holes in an infinite sheet

9 figures

## 1 INTRODUCTION

Discussions of "notch effect" and "size effect" on the fatigue limit usually include some reference to the significance of the stress gradient at the notch root. The stress gradient is generally associated with a fairly steep decrease of stress below the material surface. However, along the surface of the material at the root notch the stress is also decreasing. Even more, this decrease occurs much slower. This aspect is the main subject of the present paper. First some general comments are made on the significance of stress gradients for the notch effect. Then calculated results on stress gradients are presented. Finally the meaning of the results for considering notch and size effects is briefly discussed.

## 2 THE NOTCH EFFECT AND STRESS GRADIENTS

The prediction of the fatigue limit ( $N = \infty$ ) of a notched element under zero mean stress is a wellknown problem discussed in all textbooks on fatigue (e.g.[1]). The usual procedure is to derive the fatigue limit of the notched element ( $S_{fK}$ ) from the fatigue limit of the unnotched material ( $S_{f1}$ ). The fatigue strength reduction factor  $K_f$  (also referred to as fatigue notch factor, dynamic notch factor or effective notch factor) is defined as:

$$K_f = \frac{S_{f1}}{S_{fK}} \quad (1)$$

The most simple assumption is:

$$K_f = K_t \quad (2)$$

which can be physically justified under some restrictive conditions, which are:

- (a) The material behaviour is fully elastic and hence the peak stress at the notch will be:

$$\sigma_{\text{peak}} = K_t S \quad (3)$$

where  $S$  is the nominal stress in the notched element.

- (b) Fatigue failure of the notched element will occur is  $\sigma_{\text{peak}} \geq S_{f1}$ .  
With this condition Eq. (3) can be written as:

$$S_{f1} = K_t S_{fK}$$

Combining Eqs. (1) and (4) gives Eq. (2). (4)

It is frequently observed, especially for ductile materials and high  $K_t$  values that:

$$K_f < K_t \quad \text{or} \quad S_{fK} > \frac{S_{f1}}{K_t} \quad (5)$$

This means that either condition (a) or (b) or both are not satisfied. Since the prediction of the fatigue limit is a technical problem it should not be surprising that several equations have been proposed for relations between  $K_f$  and  $K_t$  or, which is the same, between  $S_{fK}$  and  $S_{f1}$ . Some formulas, partly wellknown, are summarized in table 1. In all the equations of the table  $\rho$  is the notch root radius (Fig. 1),  $\alpha$  is the stress gradient coefficient, defined by (see Fig. 1):

$$\left( \frac{d\sigma}{dx} \right)_{x=0} = - \alpha \frac{\sigma_{\text{peak}}}{\rho} \quad (11)$$

and  $\alpha$  is a material property with the dimension of length. The value of  $\alpha$  should be characteristic for the fatigue notch sensitivity of a material. For  $\alpha \rightarrow 0$  all equations (6) - (10) reduce to  $S_{fK} = S_{f1}/K_t$  or to  $K_f = K_t$ , which implies maximum theoretical notch sensitivity. The same result is obtained for all equations if  $\rho$  becomes very large.



Table 1:

Authors	$K_f - K_t$ relations	Corresponding $S_{fK} - S_{f1}$ relation
Neuber [2]	$q = \frac{K_f - 1}{K_t - 1} = \frac{1}{1 + \sqrt{\frac{\alpha}{\rho}}} \quad (6a)$	$S_{fK} = \frac{S_{f1}}{K_t} \left( \frac{1 + \sqrt{\frac{\alpha}{\rho}}}{1 + \frac{1}{K_t} \sqrt{\frac{\alpha}{\rho}}} \right) \quad (6)$
Siebel and Stieler [3]	$\frac{K_t}{K_f} = 1 + \sqrt{\chi} = 1 + \sqrt{\frac{\alpha \alpha}{\rho}} \quad (7a)$	$S_{fK} = \frac{S_{f1}}{K_t} \left( 1 + \sqrt{\frac{\alpha \alpha}{\rho}} \right) \quad (7)$
Peterson [4]	$q = \frac{K_f - 1}{K_t - 1} = \frac{1}{1 + \frac{\alpha}{\rho}} \quad (8a)$	$S_{fK} = \frac{S_{f1}}{K_t} \left( \frac{1 + \frac{\alpha}{\rho}}{1 + \frac{1}{K_t} \frac{\alpha}{\rho}} \right) \quad (8)$
Peterson [4]	$\frac{K_f}{K_t} = 1 - \frac{\alpha \alpha}{\rho} \quad (9a)$	$S_{fK} = \frac{S_{f1}}{K_t} \left( \frac{1}{1 - \frac{\alpha \alpha}{\rho}} \right) \quad (9)$
Heywood [5]	$\frac{K_f}{K_t} = \frac{1}{1 + 2 \sqrt{\frac{\alpha}{\rho}}} \quad (10a)$	$S_{fK} = \left( 1 + 2 \sqrt{\frac{\alpha}{\rho}} \right) \quad (10)$

The rational background of the formula's in table 1 is rather meagre. Neuber [2] argued that the peak stress itself is not conclusive with respect to the notch effect, especially so far sharp notches with steep stress gradients. With reference to the "non-homogenous, granular structure" of the material he proposed to adopt an average tensile stress in a small "elementary block" of dimension  $\epsilon$  (Fig. 1). However, equation (6) can not be obtained from this assumption and the

equation apparently has a heuristic nature. Kuhn and Hardrath [6, 7] found Neuber's equation to be in good agreement with empirical evidence. They also found that  $\alpha$  is material dependent. For steels  $\alpha$  decreased for increasing tensile strength, thus illustrating the increased notch sensitivity.

Peterson [4] considered the stress  $\sigma_y$  at a small constant depth ( $\delta = \alpha$ ) below the material surface at the notch root. This stress should be equal to the unnotched fatigue limit ( $S_{f1}$ ) to arrive at the fatigue limit of the notched element ( $S_{fK}$ ). Peterson approximated  $\sigma_y(x)$  (Fig. 1) for small values of  $x$  by a linear relation with a slope given in Eq. (11). Then equation (9) is easily obtained. In spite of this background Peterson prefers his Eq. (8) which was simply based on matching empirical evidence. The latter equation has some similarity to Neuber's equation. Replacing  $\sqrt{a/\rho}$  in Eq. (8) by  $\alpha/\rho$  gives Eq. (6). Also Peterson recognized that  $\alpha$  should depend on the type of material and its tensile strength.

Heywood [5] associated  $\alpha$  in his Eq. (10) with the length of an "equivalent inherent flaw". Nevertheless also his equation should be considered to be of an empirical nature. Heywood compared the applicabilities of his equation and Neuber's equation to empirical evidence also used by Kuhn and Hardrath. It is interesting that he found both equations to be equally useful.

Siebel and Stieler [3] fully recognized the significance of both the peak stress and the stress gradient. They defined the relative stress gradient

$$\chi = \left[ \frac{d(\sigma_y/\sigma_{\text{peak}})}{dx} \right]_{x=0} \quad (12)$$

For a certain peak stress  $\chi$  gives a direct indication on the gradient of the stress below the material surface. It seems reasonable that a steep gradient is more favourable than a low gradient. Siebel and

Stieler then postulate that the allowable peak stress ( $K_t S_{fK}$ ) as related to the unnotched fatigue strength ( $S_{f1}$ ) is a function of  $\chi$ :

$$K_t S_{fK}/S_{f1} = K_t/K_f = f(\chi) \quad (13)$$

This function should depend on the material and the relation given in Eq. (7a) was proposed for this purpose. The material constant  $\alpha$  was associated with a dimension of slip lines. Once again, there are no rational arguments to arrive at Eq. (7a), but they were in good agreement with empirical evidence. For tension and bending the variability of the stress gradient coefficient  $\alpha$  is fairly small. It is noteworthy that for a constant  $\alpha$  Eq. (7) becomes essentially equal to Heywood's equation (10). Apparently different formula's indicate the trends of effects of  $K_t$  and  $\rho$  on the fatigue limit reasonably well. However, the arguments why this is true are not very clear.

### 3 NOTCH EFFECT, SIZE EFFECT AND DIFFERENT STRESS GRADIENTS

It is easily recognized that the stress gradient at the notch root should be significant. A sharp gradient will imply a less severe situation than a low gradient. Physical explanations can be based on two different types of arguments:

(1) Plasticity effects

(2) Volume of highly stressed material with potential crack nuclei.

Plastic deformations will depend on the stress gradient, but this question will not further be considered here, since it seems less applicable to high strength material and notches with generous radii. However, the second type of argument is of great interest, because it is also associated with size effects apart from the notch effect. Tests on hole notched specimens [8, 9] showed a systematic size effect for a constant  $K_t$  value. For unnotched material the picture about size effects is less clear [10].

An analysis of size effects and stress gradient effects on the fatigue limit should start with the question: what are the potential crack nuclei, the weak spots for fatigue? Two statements often heard in this respect are:

- (a) fatigue cracks always start at the material surface
- (b) fatigue cracks usually start at some kind of an inclusion.

There is evidence for both which illustrates that the answer will depend on the type of material and the surface conditions including surface roughness. If cracks start at inclusions, they will do so in a notched element rather close to the surface in view of the higher stress. The stress gradient in Figure 1 (Eq. 11) will be important. However, if cracks start at the free surface or at inclusions close to surface the area of the highly stressed surface along the notch should be more significant. In other words stress gradients along the material surface at the notch root should be of interest. Stress distributions along the material surface will show a real maximum at the notch root, see Figure 2, with a zero stress gradient, contrary to the picture in Figure 1. In order to define the highly stressed area it will be necessary to indicate a  $y$ -coördinate where the stress along the edge of the notch has dropped a certain amount still to be specified. In Figure 3 a line of constant maximum principal stress ( $S_1$ ) is schematically indicated:

$$S_1 = \gamma \sigma_{\text{peak}} \quad (\gamma < 1) \quad (14)$$

The line intersects the  $x$ -axis at  $x = d_1$  and the notch edge at a point for which  $y = d_2$ . The  $x$ -value of the latter point will be much smaller than  $d_2$  as long as  $\gamma$  is still fairly close to one, as will be shown later. The ratio

$$\frac{d_2}{d_1} = f(\gamma) \quad (15)$$

will give an indication in which of the two directions ( $x$ -axis or

notch edge) the stress will drop more rapidly. Calculated results presented in chapter 5 will show that  $d_2/d_1$  is much larger than one for  $\gamma = 0.95$  and  $\gamma = 0.90$ . Consequently the stress variation along the notch surface may be more significant than the decrease of stress away from the surface. It is remarkable that this was hardly recognized in the literature on size effects and stress gradient effects. Papers by McClintock [11, 12] are a noteworthy exception. He studied the variation of the y-co-ordinate of the crack initiation site along the edge of a notch, and he pointed out that the variability of this co-ordinate in similar tests should have some relation to the variability of fatigue life. The meaning of the variation of the position of crack initiation for size and notch effects is obvious.

In the following chapters calculated results for  $\alpha$ ,  $d_2/d_1$  and  $S_1$  contours are presented for a variety of notches. Although such results do not solve the problem of obtaining improved  $K_f - K_t$  relations it still can shed some light on the significance of certain variables involved, which are  $K_t$ , root radius  $\rho$ , the stress gradient away from the notch and the stress variation along the notch surface.

#### 4 THE STRESS GRADIENT COEFFICIENT $\alpha$

Notches for which calculations were made are shown in Figure 4. The stress gradient coefficient  $\alpha$ , as defined in Eq.(11) and Figure 1, was previously calculated by Leven [13] for hyperbolic notches in flat bars and in round shafts. The equations were derived from the work of Neuber [2]. A recapitulation of the equations for both  $\alpha$  and  $K_t$  is given in Appendix A. Leven produced a graph showing  $\alpha$  as a function of  $\rho/d$  where  $\rho$  is the notch root radius and  $d$  is either the width or the diameter at the minimum section ( $d = 2a$  in Fig. 4). Leven's graph gives the impression that  $\alpha$  is highly variable, but this is true only if  $\rho/d$  values are considered yielding  $K_t$  values ranging from very low (close to 1) to very high (say  $K_t > 5$ ). A more relevant picture is obtained if  $\alpha$  is plotted as a function of  $K_t$ , which has been done here in Figure 5.

For an elliptical hole in an infinite sheet the well known  $K_t$  formula is (see Appendix D):

$$K_t = 1 + 2 \sqrt{\frac{a}{\rho}} \quad (16)$$

For the stress gradient coefficient the formula is also very simple (Appendix A)

$$\alpha = 2 + \frac{1}{K_t} \quad (17)$$

With these equations a line in Figure 5 for elliptical holes was obtained.

Howland [14] calculated stress distributions around a circular hole in a finite width strip and Schulz [15] did the same for an infinite sheet with an infinite row of equally spaced circular holes. In both publications data on the stress distributions in the minimum section and along the edge of the hole are presented in tabular form. From these data stress gradients were derived in Appendix B. The results are also plotted in Figure 5. The results of Howland are not fully

systematic which may be due to a limited accuracy of his calculated values. Since the stress gradient is obtained by differentiation the inaccuracy can be augmented.

Figure 5 shows that  $\alpha$  for  $K_t > 2.5$  is about 2 or slightly larger. This trend was known for a long time [e.g. 16]. For smaller  $K_t$  values larger deviations from  $\alpha \sim 2$  occur. The Howland data suggest that  $\alpha$  goes to a very high value if  $K_t$  goes to its lower limit, which is  $K_t = 2$  as shown by Koiter [17]. He obtained the latter value if the hole diameter ( $2a$ ) approaches the width of the strip ( $W$ ). For  $2a \rightarrow W$  there is still bending in the small ligaments at both sides of the hole. Consequently a high gradient in a narrow ligament should be present.

An opposite trend appears from Schulz's data where  $K_t \rightarrow 1$  for  $2a \rightarrow b$  (Fig. 4). For reasons of symmetry there is no bending in the small ligaments and an uniform stress distribution will be obtained ( $\alpha = 0$ ).

## 5 THE GRADIENT RATIO $d_2/d_1$

The coordinates  $d_1$  and  $d_2$  as defined before (Figure 3) were calculated for the same types of notches shown in Figure 4. This requires equations for the stress distributions in the minimum section and along the edge of the notch. For hyperbolic notches and elliptical holes exact equations are available which are recapitulated in Appendix C and D respectively. From the equations  $d_2$  can be solved, whereas  $d_1$  has to be obtained by iteration. For a hole in a strip (Howland [14]) and a row of holes in a plate (Schulz [15]) values of  $d_1$  and  $d_2$  were derived from the numerical data on stress distributions presented in [14] and [15] and summarized in Appendix B.

Calculations were made for  $\gamma = 0.95$ ,  $\gamma = 0.90$  and  $\gamma = 0.80$  respectively, i.e. for the locations where the main principle stress  $S$ , has dropped to 95%, 90% and 80% of  $\sigma_{\text{peak}}$ . The results given in Appendix B, C and D have been plotted in Figure 6 for  $\gamma = 0.95$  and

$\gamma = 0.90$  as a function of  $K_t$ . It is remarkable that  $d_2/d_1$  values are practically constant for  $K_t > 2$ , whereas significantly deviating values require  $K_t < 1.5$ . Apparently there is a large conformity between the various notches, independent of the severity of the notch.

A second observation is that  $d_2/d_1$  is fairly large, the average being 8.3 for  $\gamma = 0.95$  and 5.6 for  $\gamma = 0.90$ . In other words the decay of stress along the notch is considerably slower than in the direction perpendicular to the surface of the material at the notch root.

## 6 STRESS DISTRIBUTIONS FOR THREE DIFFERENT HOLES

In view of the conformity noted before, lines of constant maximum principal stress ( $S_1$ ) were calculated for three holes with highly different  $K_t$  values. Elliptical holes with major to minor axis ratio 3, 1 and 1/3 were adopted for which  $K_t$  is 7, 3 and 1.67 respectively. Equations are compiled in Appendix D, where the calculated results are presented in tabular form. The data are plotted in Figure 7a - c. The similarity is obvious already from comparing these Figures, but a more easy comparison can be made in Figure 8, where the same lines of constant maximum principal stress are shown. In Figure 8 the scales adopted were chosen to have the same absolute  $\rho$  value in all three cases. The line for  $\gamma = 0.95$  has been dropped in Figure 8 for clarity. It is surprising to see the similarity between the constant  $\gamma$ -lines for  $\gamma = 0.90$  and  $\gamma = 0.80$  for three highly different notch severities.

## 7 DISCUSSION

### 7.1 Evaluation of the calculated results

At the root of a notch the highest stress  $\sigma_{\text{peak}}$  occurs at a single point only (or a single line). The stress decreases away from the material surface (Fig. 1), while it also decreases along the surface away from the point where  $\sigma_{\text{peak}}$  applies (Fig. 2). However, in the



latter direction the decrease does not start with a steep gradient, and it requires a larger distance for a 5 or 10 percent decrease of stress. This fact is easily observed from photo-elastic pictures, but its significance for notch and size effects was not generally recognized.

The present calculations confirm that  $d_2/d_1$  (Fig. 3) for  $S_1/\sigma_{\text{peak}} = 0.95$  or  $0.90$  is fairly large (Fig. 6), while it turns out to be approximately constant for a considerable variation of  $K_t$ . The distance  $d_1$  away from the notch surface is obviously related to the stress gradient as expressed in Eq. (8) (see also Fig. 1):

$$\left(\frac{d\sigma_y}{dx}\right)_x = 0 \quad \sim \quad \frac{\Delta\sigma}{d_1} = - \frac{(1 - \gamma) \sigma_{\text{peak}}}{d_1} \quad (18)$$

The latter equality follows from the definition of  $\gamma$  in Equation (14) Combining Eqs (11) and (18) gives

$$d_1 \sim \rho \frac{(1 - \gamma)}{\alpha} \quad (19)$$

For  $K_t > 2$  the variation of  $\alpha$  is rather small (Fig. 5) and Eq. (19) then implies that  $d_1/\rho$  is approximately constant, irrespective of the severity of the notch. A characteristic value of  $\alpha$  is in the order of 2.3, ignoring both very small  $K_t$  values and large  $K_t$  values. Consequently a 5 percent drop of stress ( $\gamma = 0.95$ ) is then obtained according to Eq. (19) at:

$$d_1/\rho \sim 2.2 \text{ percent} \quad (20)$$

In other words: At a distance of about 2 percent of the root radius below the notch root surface the stress has decreased with 5 percent as compared to the peak stress at root surface. This result is independent of the  $K_t$  factor within certain limits mentioned before.

The tendency for a constant  $d_2/d_1$  (Fig. 6) implies that  $d_2/\rho$  will also be approximately constant. With an average value of  $d_2/d_1$  of 8.3 for  $\gamma = 0.95$

$$d_2/\rho \sim 18 \text{ percent} \quad (21)$$

In other words: a 5 percent decrease of stress along the surface of the root notch material occurs at a distance to the minimum section of about 18 percent of the root radius, irrespective of the severity of the notch within limits mentioned before.

Similar to Eqs (18) we can write for the stress variation along the surface

$$\frac{\Delta\sigma}{d_2} = - \frac{(1 - \gamma) \sigma_{\text{peak}}}{d_2} \quad (22)$$

In analogy to Eq. (11) a second stress gradient coefficient can be defined by

$$\frac{\Delta\sigma}{d_2} = - \beta \frac{\sigma_{\text{peak}}}{\rho} \quad (23)$$

which gives:

$$\beta = \frac{\rho}{d_2} (1 - \gamma) \quad (24)$$

The tendency for a constant  $\rho/d_2$  should also appear from  $\beta$  values calculated with Eq. (24). Such values are plotted in Figure 9 for  $\gamma = 0.95$ . Although systematic effects are apparent it turns out that the variation of  $\beta$  for  $K_t > 2$  is relatively small.

## 7.2 Characterisation of the notch severity

The peak stress is obtained as the product of  $K_t$  and the normal stress, where  $K_t$  is depending on the shape of the component.  $K_t$  gives no information about stress distributions around the notch. Stress gradients in this area are closely related to the notch root radius. Relative gradients can be written as:

$$\chi = \frac{\Delta\sigma/\sigma_{\text{peak}}}{d} \quad (25)$$

which is approximately equal to  $-\alpha/\rho$  away from the material surface and to  $-\beta/\rho$  along the surface. For  $K_t$  from 2 to 5 both  $\alpha$  and  $\beta$  show a small variation only. Consequently the absolute size of the root radius gives a first and predominant impression of the stress gradients. This is also illustrated by Figure 8. The implication is that the same  $\rho$  gives approximately the same relative stress gradient  $\chi$ . The highly stressed region is therefore characterized by two factors:  $K_t$  and  $\rho$  or  $K_t$  and  $\chi$ .

Some limitations of the present calculations should be mentioned here. Torsion as a loading mode has not been analysed. It is known that  $\alpha$  values usually are much smaller than for tension. For bending only a few results were calculated here which show similar results as for tension. It is expected that the small variability of  $\alpha$  and  $\beta$  will be apply to bending in general.

### 7.3 $K_f - K_t$ relations

Obviously the previous discussion does not solve the problem of a  $K_f - K_t$  relation, because the basic model for such a relation is still lacking. However, from the small variability of  $\alpha$  and  $\beta$  it can be concluded that  $K_t$  and  $\rho$  are characterising the severity of the local stress level, the stress gradient and the volume of highly stress material. In  $K_f - K_t$  relations no more than these two dimension-parameters seem to be required. The problem is how to include the fatigue resistance of the material. From the work of McClintock it follows that both the fatigue resistance per se and its statistical nature should be introduced in a model for obtaining a rational  $K_f - K_t$  relation. Unfortunately with the present knowledge about crack initiation sites there is little hope to arrive at a generally applicable model. For the time being empirical rules have to be used. Furthermore, due consideration should be given to the relevance of

the basic fatigue data for the fatigue problem for which predictions have to be made. In particular similar surface quality and material structure should be aimed at.

## 8 CONCLUSIONS

1. Stress gradients at the root of a notch are significant for the notch effect and the size effect on the fatigue limit. Usually the gradient of the stress distribution in the minimum section is considered. However, calculations have shown that the stress is decreasing much slower along the surface of the material at the notch root. Below the surface of the notch the stress in the minimum section has dropped to 95 percent of  $\sigma_{\text{peak}}$  at a distance of about 2 percent of the notch root radius. Along the material surface the distance for the same reduction in stress is about 18 percent of the notch root radius. These percentages turn out to be fairly independent of  $K_t$  in the range of  $K_t$  values from 2 to 5.
2. For the same  $K_t$  and root radius  $\rho$  there is a striking quantitative similarity between the stress distributions around the notch root. This conclusion was borne out by calculations for several notches loaded in tension and one notch loaded in bending. It probably will apply to bending in general. No calculations were made for torsion.
3. Since  $K_t$  and  $\rho$  fairly well characterize the stress conditions of the notch root both variables should enter in prediction rules for the fatigue limit of a notched element. In view of lack of knowledge about crack nucleation sites and the variability of the sites it is difficult to arrive at rational prediction rule. Existing empirical rules have to be adopted.

## 9 REFERENCES

- [1] N.E. Forst, K.J. Marsh and L.P. Pook: Metal Fatigue. Clarendon Press, Oxford 1974.
- [2] H. Neuber: Kerbspannungslehre. Springer Verlag, 1937 (2nd ed. 1958) (Translation: Theory of Notch Stresses, Edwards, London 1946).
- [3] E. Siebel and M. Stieler: Ungleichförmige Spannungsverteilung bei schwingender Beanspruchung. Zeitschrift VDI, Vol. 97, 1955, p. 121.
- [4] R.E. Peterson: Notch-sensitivity. Metal Fatigue, ed. by G. Sines and J.L. Waisman, McGraw-Hill, New York 1959, p. 293.
- [5] R.B. Heywood: Stress concentration factors. Relating theoretical and practical factors in fatigue loading. Engineering, Vol. 179, 1955, p. 146.
- [6] P. Kuhn and H.F. Hardrath: An engineering method for estimating notch-size effect in fatigue tests on steel. NACA TN 2805, 1952.
- [7] P. Kuhn: Effect of geometric size on notch fatigue. Colloquium on Fatigue, Stockholm 1955. Ed. by W. Weibull and F.K.G. Odquist. Springer Verlag 1956, p. 131.
- [8] C.B. Landers and H.F. Hardrath: Results of axial load fatigue tests on electro-polished 2024-T3 and 7075-T6 aluminum alloy sheet specimens with central holes. NACA TN 3631, 1956.
- [9] C.E. Philips and R.B. Heywood: Size effect in fatigue of plain and notched steel specimens loaded under reversed direct stress. Proc. Instn. Mech. Engrs, Vol. 165, 1951, p. 113.
- [10] R.B. Heywood: Designing against fatigue. Chapman and Hall, London 1962.
- [11] F.A. McClintock: The statistical theory of size and shape effects in fatigue. J. Appl. Mech., Vol. 22, 1955, p. 421.

- [12] F.A. McClintock: Variability in fatigue testing: Sources and effect on notch sensitivity. Colloquium on Fatigue, Stockholm 1955. Ed. by W. Weibull and F.K.G. Odquist. Springer Verlag, 1956, p. 171.
- [13] M.M. Leven: Stress gradients in grooved bars and shafts. Proc.SESA, Vol. 13, 1955, p. 207.
- [14] R.C.J. Howland: On the stresses in the neighbourhood of a circular hole in a strip under tension. Phil. Trans. Roy. Soc. (London), Vol. 229, 1929-1930, p. 49.
- [15] K.J. Schulz: Over de spanningstoestand in doorboorde platen (On the stresses in plates with holes). Delft Un. of Tech., doctor thesis, 1941.
- [16] C.S. Yen and T.J. Dolan: A critical review of the criteria for notch-sensitivity in fatigue of metals. Un. of Illinois, Eng. Exp. Station, Bulletin Series No. 398, 1952.
- [17] W.T. Koiter: An elementary solution of two stress concentration problems in the neighbourhood of a hole. Quart. Appl. Math., Vol. 15, 1957, p. 303.
- [18] S. Timoshenko and J.N. Goodier: Theory of elasticity, 2nd ed. McGraw-Hill, New York 1951.

APPENDIX A: THE STRESS GRADIENT COEFFICIENT  $\alpha$  AND  $K_t$  FOR HYPERBOLIC NOTCHES AND AN ELLIPTICAL HOLE

Hyperbolic notches:

$K_t$ -equations are given by Neuber in his book [2] while  $\alpha$  values are easily derived from equations in that book.

Flat bar tension:

$$K_t = \frac{2 \left(1 + \frac{a}{\rho}\right) \sqrt{\frac{a}{\rho}}}{\left(1 + \frac{a}{\rho}\right) \operatorname{arc} \operatorname{tg} \sqrt{\frac{a}{\rho}} + \sqrt{\frac{a}{\rho}}} \quad (\text{A1})$$

$$\alpha = 2 \quad (\text{A2})$$

Shaft, tension:

$$K_t = \frac{\frac{a}{\rho} \sqrt{\frac{a}{\rho} + 1} + (0.5 + \nu) \frac{a}{\rho} + (1 + \nu) \left( \sqrt{\frac{a}{\rho} + 1} + 1 \right)}{\frac{a}{\rho} + 2\nu \sqrt{\frac{a}{\rho} + 1} + 2} \quad (\text{A3})$$

$$\alpha = \frac{4 \frac{a}{\rho} - (1 - 2\nu) \sqrt{1 + \frac{a}{\rho}} + 5}{2 \frac{a}{\rho} - (1 - 2\nu) \sqrt{1 + \frac{a}{\rho}} + 3} \quad (\text{A4})$$

Flat bar, bending:

$$K_t = \frac{4 \frac{a}{\rho} \sqrt{\frac{a}{\rho}}}{3 \left[ \sqrt{\frac{a}{\rho}} + \left( \frac{a}{\rho} - 1 \right) \operatorname{arc} \operatorname{tg} \sqrt{\frac{a}{\rho}} \right]} \quad (\text{A5})$$

$$\alpha = 2 + \frac{\rho}{a} \quad (\text{A6})$$

Shaft, bending:

$$K_t = \frac{\frac{3}{4} \left( \sqrt{\frac{a}{\rho} + 1} + 1 \right) \left[ 3 \frac{a}{\rho} - (1 - 2\nu) \sqrt{\frac{a}{\rho} + 1} + 4 + \nu \right]}{3 \left( \frac{a}{\rho} + 1 \right) + (1 + 4\nu) \sqrt{\frac{a}{\rho} + 1} + \frac{1 + \nu}{1 + \sqrt{\frac{a}{\rho} + 1}}} \quad (A7)$$

$$\alpha = \left( 1 + \frac{\rho}{a} \right) \left[ \frac{6 - (1 - 2\nu) \sqrt{\frac{\rho}{a}} \sqrt{1 + \frac{\rho}{a}} + (4 + \nu) \frac{\rho}{a}}{3 - (1 - 2\nu) \sqrt{\frac{\rho}{a}} \sqrt{1 + \frac{\rho}{a}} + (4 + \nu) \frac{\rho}{a}} \right] \quad (A8)$$

Elliptical hole:

$$K_t = 1 + 2 \frac{a}{b} = 1 + 2 \sqrt{\frac{a}{\rho}} \quad (A9)$$

The stress gradient coefficient  $\alpha$  is obtained by differentiation of Eq. (C4) which leads to:

$$\alpha = \frac{3 + 4 \frac{a}{b}}{1 + 2 \frac{a}{b}} = 2 + \frac{1}{K_t} \quad (A10)$$



APPENDIX B: STRESS GRADIENTS AROUND CIRCULAR HOLES ACCORDING TO THE  
STUDIES OF HOWLAND AND SCHULZ

The results of Howland

Howland [14] calculated stress distributions in a finite width strip with a central circular hole. Relevant data of [14] are reproduced here in table B1. The lower figure in the table did not occur in Howland's original paper, but it was added later (see [14] page 82) because he was suggested to do so. It is surprising that this figure is not a very accurate representation of table B1. Stress gradients will be derived here from the data in the table.

For a circular hole (radius  $a$ ) in an infinite plate the exact solution for  $\sigma_y$  along the X-axis is [18]:

$$\frac{\sigma_y}{S} = 1 + \frac{1}{2} \left(\frac{a}{x}\right)^2 + \frac{3}{2} \left(\frac{a}{x}\right)^4 \quad (B1)$$

It is assumed that for a finite width a relation of the same type can be used to approximate the stress distribution:

$$\frac{\sigma_y}{S} = A + B \left(\frac{a}{x}\right)^2 + C \left(\frac{a}{x}\right)^4 \quad (B2)$$

The stress gradient at the edge of the hole is:

$$\left(\frac{d(\sigma_y/S)}{dx}\right)_{x=a} = - \frac{(2B + 4C)}{a} \quad (B3)$$

A, B and C were obtained by using three  $\sigma_y$  values from table B1 as close to the edge of the hole as possible, which includes one point on the edge of the hole. The results are presented in table B1 including  $\alpha$  and  $K_t$  values. The coefficient  $\alpha$  was defined before by:

$$\left(\frac{d\sigma_y}{dx}\right)_{\text{edge of hole}} = -\alpha \frac{\sigma_{\text{peak}}}{\rho} = -\alpha \frac{(A + B + C) S}{a} \quad (\text{B4})$$

where the root radius  $\rho = a$ . The value of  $K_t$  follows from

$$K_t = \sigma_{\text{peak}}/\sigma_{\text{nominal}} \quad \text{with} \quad \sigma_{\text{nominal}} = \frac{W}{W - a} S \quad (\text{B5})$$

Combining Eqs. (B4) and (B5) gives:

$$\alpha = \frac{2B + 4C}{A + B + C} \quad (\text{B6})$$

The distance  $d_1 (= a_1 - a)$  where  $\sigma_y$  along the X-axis has dropped to  $\gamma\sigma_{\text{peak}}$  ( $\gamma \leq 1$ ,  $\sigma_{\text{peak}}/S = A + B + C$ ) is easily obtained from Eq. (B2):

$$\gamma(A + B + C) = A + B \left(\frac{a}{a_1}\right)^2 + C \left(\frac{a}{a_1}\right)^4 \quad (\text{B7})$$

Calculated results are given in table B3.

Along the edge of the hole Howland presents the tangential stress  $\sigma_\eta$  for some values of  $\eta$ , which for the lowest  $\eta$  values are reproduced here in table B2. For  $a/W = 0$  (infinite sheet)  $\sigma_\eta$  is given by:

$$\frac{\sigma_\eta}{S} = 1 + 2 \cos 2\eta = -1 + 4 \cos^2 \eta \quad (\text{B8})$$

For a finite width an interpolation of the following type is adopted:

$$\frac{\sigma_\eta}{S} = A + B \cos \eta + C \cos^2 \eta \quad (\text{B9})$$

It satisfies the zero gradient for  $\eta = 0$ . Constants A, B and C were then calculated from the  $\sigma_\eta$  values in table B2. Subsequently the y-coordinate  $d_2$  where  $\sigma_\eta$  has dropped to  $\gamma\sigma_{\text{peak}}$  is obtained as  $d_2 = \sin \eta$  with  $\eta$  following from:

$$\gamma(A + B + C) = A + B \cos \eta + C \cos^2 \eta \quad (B10)$$

Calculated values are presented in table B3, where the ratio  $d_2/d_1$  is given also.

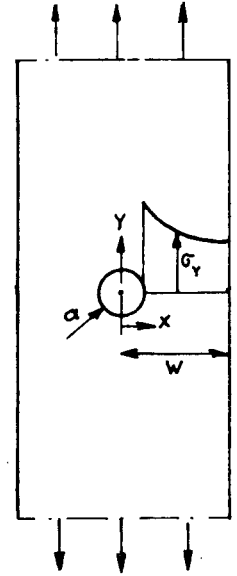
The results show that the effect of  $a/W$  on  $\alpha$ ,  $d_1$ ,  $d_2$  and  $d_2/d_1$  is slightly inconsistent, which should be associated with a limited accuracy of Howland's data. Values of  $\alpha$  and  $d_1/d_2$  have been plotted in Figures 5 and 6.

#### The results of Schulz

Schulz [15] analysed an infinite sheet with an infinite row of co-linear holes, see the figure in table B4. Since he presented his data in a similar form as Howland the equations (B2) to (B10) could be adopted again. The results as compiled in tables B4 to B6 again show some slight inconsistencies, but to a lesser degree as for Howland's results. Values of  $\alpha$  and  $d_1/d_2$  have been plotted in Figures 5 and 6.

Table B1. Data of Howland and calculated  $\alpha$ -values.

$\frac{x}{W}$	$\sigma_y/S$				
	$\frac{a}{W} = 0.1$	$\frac{a}{W} = 0.2$	$\frac{a}{W} = 0.3$	$\frac{a}{W} = 0.4$	$\frac{a}{W} = 0.5$
0.1	<u>3.03</u> (*)				
0.2	<u>1.23</u> (*)	<u>3.14</u> (*)			
0.3	<u>1.08</u> (*)	<u>1.57</u> (*)	<u>3.36</u> (*)		
0.4	<u>1.04</u>	<u>1.26</u> (*)	<u>1.93</u> (*)	<u>3.74</u> (*)	
0.5	<u>1.03</u>	<u>1.16</u>	<u>1.47</u> (*)	<u>2.30</u> (*)	<u>4.32</u> (*)
0.6	<u>1.02</u>	<u>1.11</u>	<u>1.28</u>	<u>1.75</u> (*)	<u>2.75</u> (*)
0.7	<u>1.01</u>	<u>1.07</u>	<u>1.17</u>	<u>1.48</u>	<u>2.04</u> (*)
0.8	<u>1.01</u>	<u>1.05</u>	<u>1.07</u>	<u>1.28</u>	<u>1.61</u>
0.9	<u>1.00</u>	<u>1.01</u>	<u>0.96</u>	<u>1.08</u>	<u>1.22</u>
1.0	<u>0.99</u>	<u>0.97</u>	<u>0.89</u>	<u>0.81</u>	<u>0.73</u>
A	1.001	1.044	0.968	1.108	1.003
B	0.544	0.454	0.835	0.494	0.694
C	1.485	1.642	1.558	2.138	2.623
$\alpha$	2.32	2.38	2.35	2.55	2.75
$K_t$	2.73	2.51	2.35	2.24	2.16



(\*) These values were used to calculate A, B and C.  
Underlined values are  $\sigma_{\text{peak}}/S$  values at edge of hole.

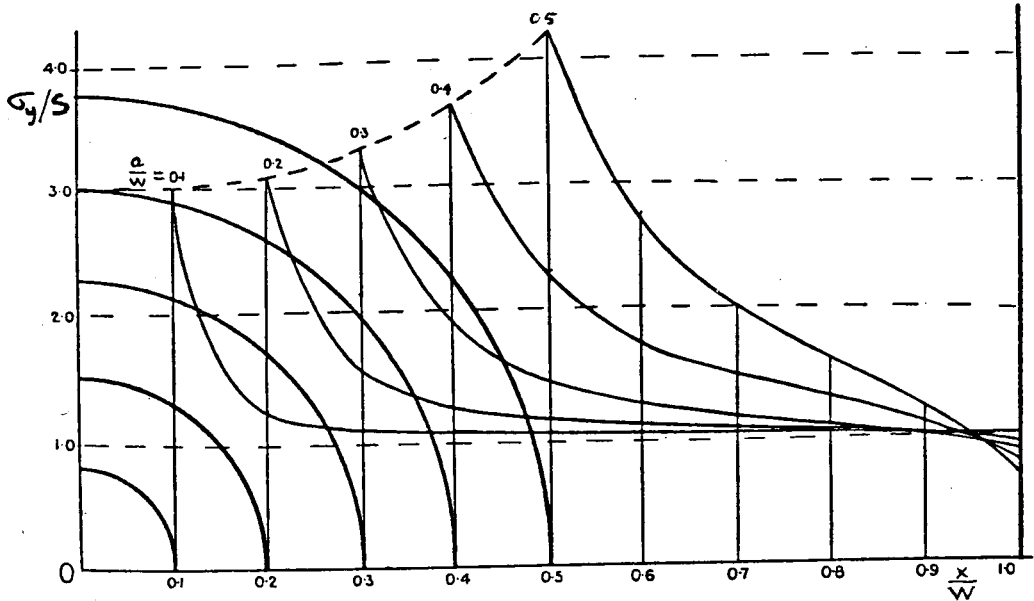


Table B2. Numerical data of Howland.

$\eta$	$\sigma_{\eta}/S$					
	$\frac{a}{W} = 0$	$\frac{a}{W} = 0.1$	$\frac{a}{W} = 0.2$	$\frac{a}{W} = 0.3$	$\frac{a}{W} = 0.4$	$\frac{a}{W} = 0.5$
0	3.00	3.03	3.14	3.36	3.74	4.32
15°	2.73	2.74	2.85	3.03	3.32	3.72
30°	2.00	2.00	2.07	2.15	2.25	2.32
A	-0.478	3.197	-0.302	-0.009	3.060	12.628
B	-1.124	-9.150	-1.806	-3.169	-11.378	-35.139
C	4.602	8.984	5.248	6.538	12.057	26.831

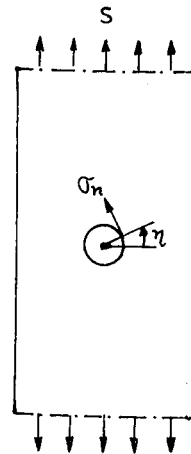
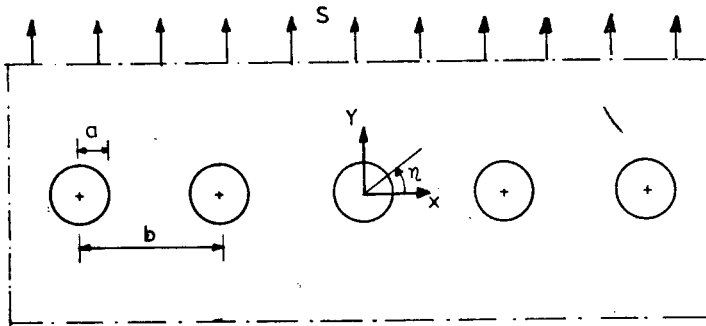


Table B3. Calculated results derived from Howland's data.

$a/W$	$K_t$	$\gamma = 0.95$			$\gamma = 0.90$			$\gamma = 0.80$			$\beta(\gamma=0.95)$ (Eq. 24)
		$d_1/a$	$d_2/a$	$d_2/d_1$	$d_1/a$	$d_2/a$	$d_2/d_1$	$d_1/a$	$d_2/a$	$d_2/d_1$	
0(*)	3	0.0226	0.194	8.6	0.048	0.274	5.7	0.109	0.387	3.6	0.257
0.1	2.73	0.0227	0.186	8.2	0.048	0.265	5.5	0.109	0.378	3.5	0.269
0.2	2.51	0.0221	0.190	8.6	0.047	0.269	5.7	0.106	0.382	3.6	0.263
0.3	2.35	0.0224	0.184	8.2	0.047	0.261	5.6	0.107	0.371	3.5	0.272
0.4	2.24	0.0206	0.172	8.3	0.043	0.244	5.7	0.097	0.348	3.6	0.291
0.5	2.16	0.0190	0.154	8.1	0.040	0.219	5.5	0.089	0.313	3.5	0.325

(\*) Exact solution.

Table B4. Numerical data from Schulz and calculated  $\alpha$ -values.

$\frac{x}{b}$	$\sigma_y/S$			
	$\frac{a}{b} = 0.10$	$\frac{a}{b} = 0.15$	$\frac{a}{b} = 0.20$	$\frac{a}{b} = 0.25$
0.10	3.006			
0.15	1.543	3.031		
0.20	1.244	1.819	3.096	
0.25	1.143	1.441	2.072	3.241
0.30	1.099	1.287	1.665	2.357
0.40	1.065	1.175	1.380	1.739
0.50	1.057	1.150	1.321	1.612
A	1.022	1.055	1.124	1.327
B	0.523	0.564	0.612	0.505
C	1.461	1.412	1.360	1.409
$\alpha$	2.29	2.24	2.15	2.05
$K_t$	2.40	2.12	1.86	1.62

Table B5. Numerical data from Schulz.

$\eta$	$\sigma_{\eta}/S$			
	$a/b = 0.10$	$a/b = 0.15$	$a/b = 0.20$	$a/b = 0.25$
0	3.0063	2.0309	3.0962	3.2410
10°	2.8925	2.9199	2.9936	3.1485
20°	2.5540	2.5989	2.6928	2.8686
30°	2.0387	2.1024	2.2175	2.4068
A	-4.686	-1.153	-2.252	-4.734
B	7.897	1.013	3.921	9.890
C	-0.205	3.171	1.427	-1.915

Table 6. Calculated results derived from Schulz's data.

$a/b$	$K_t$	$\gamma = 0.95$			$\gamma = 0.90$			$\gamma = 0.80$			$\beta(\gamma=0.95)$ (Eq. 24)
		$d_1/a$	$d_2/a$	$d_2/d_1$	$d_1/a$	$d_2/a$	$d_2/d_1$	$d_1/a$	$d_2/a$	$d_2/d_1$	
0(*)	3.00	0.0226	0.1936	8.6	0.0478	0.2739	5.7	0.1086	0.3873	3.6	0.258
0.10	2.40	0.0230	0.1993	8.7	0.0487	0.2804	5.8	0.1110	0.3922	3.5	0.251
0.15	2.12	0.0236	0.2029	8.6	0.0501	0.2867	5.7	0.1144	0.4048	3.5	0.246
0.20	1.86	0.0246	0.2131	8.7	0.0522	0.3003	5.8	0.1198	0.4216	3.5	0.235
0.25	1.62	0.0259	0.2288	8.8	0.0552	0.3201	5.8	0.1284	0.4432	3.5	0.219

(\*) exact solution

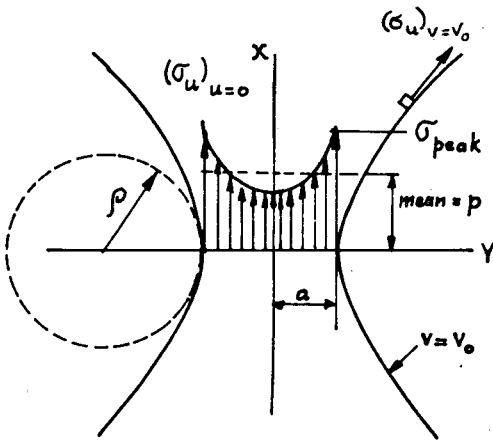




## APPENDIX C: STRESS DISTRIBUTIONS AROUND HYPERBOLIC NOTCHES IN INFINITE MATERIAL

The equations for hyperbolic notches were derived by Neuber in his book "Kerbspannungslehre" [2]. The symbols used in his book are largely maintained here.

### Flat bar in tension



The elliptical co-ordinates  $u$  and  $v$  are related to the Cartesian co-ordinates by:

$$x = c \sinh u \cos v \quad (C1a)$$

$$y = c \cosh u \sin v \quad (C1b)$$

The hyperbolic notch is given by  $v = v_0$  or:

$$\left(\frac{y}{a}\right)^2 - \left(\frac{x}{b}\right)^2 = 1 \quad (C2)$$

where

$$a = c \sin v_0, \quad b = c \cos v_0 \quad (C3)$$

In the minimum section and along the edge of the notch the stresses are given by:

$$(\sigma_u)_{u=0} = \frac{A}{\cos v} \left[ 1 + \frac{\cos^2 v_0}{\cos^2 v} \right] \quad (C4)$$

$$(\sigma_u)_{v=v_0} = \frac{2A \cosh u \cos v_0}{\cosh^2 u - \sin^2 v_0} \quad (C5)$$

where

$$A = \frac{p \sin v_0}{v_0 + \sin v_0 \cos v_0} \quad (C6)$$

and

$$\cos v_0 = \left(1 + \frac{a}{\rho}\right)^{-1/2} \quad (C7)$$

Note that the notch severity is fully described by the ratio  $a/\rho$ . Substitution of  $v = v_0$  in Eq. (C4) or  $u = 0$  in Eq. (C5) gives:

$$K_t = \frac{\sigma_{\text{peak}}}{p} = \frac{2A}{p \cos v_0} \quad (C8)$$

The distance  $d_1 = a - y$  along the Y-axis where  $(\sigma_u)_{u=0}$  has dropped to  $\gamma\sigma_{\text{peak}}$  then follows from:

$$\gamma = \frac{(\sigma_u)_{u=0}}{\sigma_{\text{peak}}} = \frac{1}{2} \frac{\cos v_0}{\cos v} \left[ 1 + \frac{\cos^2 v_0}{\cos^2 v} \right] \quad (C9)$$

Cos  $v$  for a specific value of  $\gamma$  is found by iteration and the corresponding value of  $y$  follows from Eqs. (C1b) ( $u = 0$ ) and (C3):

$$\frac{y}{a} = \frac{\sin v}{\sin v_0} \quad (C10)$$

Calculated results of  $d_1/a = 1 - y/a$  are presented in table C1.

Similarly along the edge of the notch ( $v = v_0$ ):

$$\gamma = \frac{(\sigma_u)_{v=v_0}}{\sigma_{\text{peak}}} = \frac{\cosh u \cos^2 v_0}{\cosh^2 u - \sin^2 v_0} \quad (C11)$$

Cosh  $u$  can be solved from this equation and the corresponding x-co-ordinate ( $= d_2$ ) where  $(\sigma_u)_{v=v_0}$  has dropped to  $\gamma\sigma_{\text{peak}}$  then follows

from Eqs. (C1a) ( $v = v_0$ ) and (C3):

$$\frac{x}{a} = \cot v_0 \sinh u \quad (C12)$$

Calculated results are given in table C1.

### Flat bar in bending

From Neuber's book one easily obtains:

Along the y-axis:

$$(\sigma_u)_{u=0} = 4A \operatorname{tg} v \left( 1 + \frac{\cos^2 v_0}{\cos^2 v} \right) \quad (C13)$$

where:

$$A = \frac{-p \sin^2 v_0}{3(\sin 2v_0 - 2v_0 \cos 2v_0)} \quad (C14)$$

Here p is the nominal bending stress, related to the bending moment by:

$$p = \frac{3M}{2a^2d} \quad (C15)$$

From Eq. (C13) the peak stress is obtained by putting  $v = v_0$ :

$$K_t = \frac{\sigma_{\text{peak}}}{p} = 8 \frac{A}{p} \operatorname{tg} v_0 \quad (C16)$$

Instead of Eq. (C9) the result now is:

$$\gamma = \frac{1}{2} \frac{\operatorname{tg} v}{\operatorname{tg} v_0} \left[ (1 + \cos^2 v_0) + \cos^2 v_0 \operatorname{tg}^2 v \right] \quad (C17)$$

For a specific  $\gamma$  value the corresponding  $\operatorname{tg} v$  is obtained by iteration, and the value of  $d_1$  where  $\gamma_1$  applies then follows from Eq. (C10).

Along the edge of the notch:

$$(\sigma_u)_{v=v_0} = \frac{8A \sin v_0 \cos v_0}{\cosh^2 u \sin^2 v_0} \quad (C18)$$

and:

$$\gamma = \frac{(\sigma_u)_{v=v_0}}{p} = \frac{\cos^2 v_0}{\cosh^2 u \sin^2 v_0} \quad (C19)$$

After solving  $\cosh u$  for a specific value of  $\gamma$  Eq. (C12) applies to find the corresponding  $d_2$  value.

Numerical data are presented in table C1.

#### Round bar in tension

Equations (C1) - (C3) and (C7) still apply. Stresses in the minimum section and along the edge of the notch are:

$$(\sigma_u)_{u=0} = \frac{C}{\cos v} \left[ \cos^2 v_0 - (1 - 2\nu) \cos v_0 + 1 + \left( \frac{\cos v_0}{\cos v} \right)^2 \right] \quad (C20)$$

$$(\sigma_u)_{v=v_0} = C \left[ \frac{\cos v_0 \{ \cos^2 v_0 - (1 - 2\nu) \cos v_0 + 2 \} - (1 - 2\nu - 3 \cos v_0) \sinh^2 u}{(1 + \sinh^2 u) (\sinh^2 u + \cos^2 v_0)} \right] \quad (C21)$$

where:

$$C = -\frac{p}{2} \left[ \frac{1 + \cos v_0}{1 + 2\nu \cos v_0 + \cos^2 v_0} \right] \quad (C22)$$

Substitution of  $v = v_0$  in Eq. (C20) or  $u = 0$  in Eq. (C21) leads to:

$$K_t = \frac{\sigma_{\text{peak}}}{p} = \frac{C/p}{\cos v_0} \left[ \cos^2 v_0 - (1 - 2\nu) \cos v_0 + 2 \right] \quad (C23)$$

Further in the minimum section:

$$\gamma = \frac{(\sigma_u)_{u=0}}{\sigma_{\text{peak}}} = \frac{\cos v_0}{\cos v} \left[ 1 + \frac{\left( \frac{\cos v_0}{\cos v} \right)^2 - 1}{\cos^2 v_0 - (1 - 2v) \cos v_0 + 2} \right] \quad (\text{C24})$$

and along the notch edge:

$$\gamma = \frac{(\sigma_u)_{v=v_0}}{\sigma_{\text{peak}}} = \frac{1}{\cosh^2 u} \left[ 1 - \frac{2(\cosh^2 u - 1)}{\cosh^2 u - \sin^2 v_0} \cdot \frac{(1 - \cos^2 v_0)}{\{\cos^2 v_0 - (1 - 2v) \cos v_0 + 2\}} \right] \quad (\text{C25})$$

For a specific  $\gamma$  value  $\cos v$  has to be obtained from Eq. (C24) by iteration, whereas  $\cosh u$  can be solved from Eq. (C25) directly. Corresponding values of  $d_1$  and  $d_2$  are then obtained with Eqs. (C10) and (C11). Numerical results are given in table C1. Calculations were made for  $v = 0.3$ .

### Calculated results

Values of  $d_1$  and  $d_2$  were calculated for a drop of the stress from the peak value at the notch root ( $\sigma_{\text{peak}} = K_t S$ ) with an amount of 5%, 10% and 20% respectively, corresponding to  $\gamma = 0.95$ ,  $\gamma = 0.90$  and  $\gamma = 0.80$ . The results are presented in table C1, while  $d_2/d_1$  values are plotted in Figure 6. Apparently  $d_2/d_1$  is fairly constant, except for values at low  $K_t$ . For low  $K_t$  values (obtained by  $v_0 \rightarrow 0$ ) the ratio  $d_1/d_2 \rightarrow \infty$  for bending because  $d_2/a$  goes to infinity and  $d_1/a < 1$ . For tension and low  $K_t$  values  $d_2/d_1$  is decreasing, but an asymptotic value cannot be indicated. For low  $K_t$  values and tension, the stress in the minimum section does not drop enough to give real  $d_1$  values and  $d_2/d_1$  becomes non-existent.

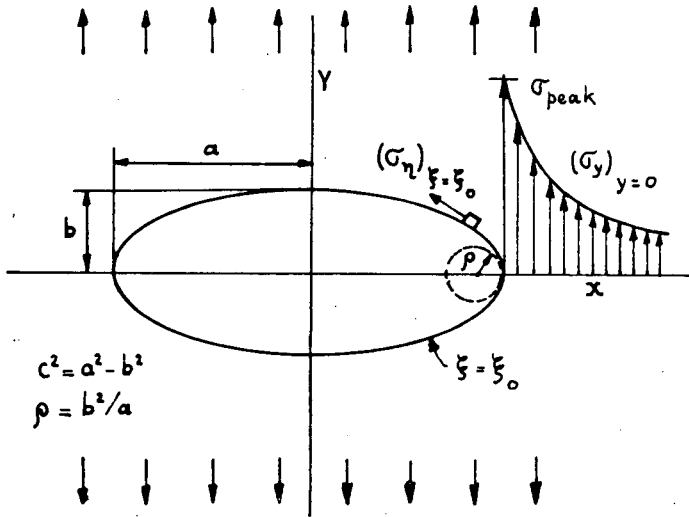
Table C1. Calculated results for hyperbolic notches.

hyperbolic notch in:	loading	$\rho/a$	$K_t$	$\gamma = 0.95$				$\gamma = 0.90$				$\gamma = 0.80$				$\beta(\gamma=0.95)$ (Eq. 24)
				$d_1/a$	$d_2/a$	$d_2/d_1$		$d_1/a$	$d_2/a$	$d_2/d_1$		$d_1/a$	$d_2/a$	$d_2/d_1$		
flat bar	tension	1/15	4.96	0.00177	0.01506	8.51		0.00376	0.02190	5.82		0.00865	0.03292	3.81		0.221
		1/9	3.87	0.00295	0.02484	8.42		0.00628	0.03615	5.76		0.01445	0.05442	3.77		0.224
		1/5	2.94	0.00531	0.04385	8.26		0.01133	0.06387	5.64		0.02617	0.09638	3.68		0.228
		1/3	2.34	0.00887	0.07105	8.01		0.01896	0.10363	5.47		0.04401	0.15688	3.56		0.235
		1/2	1.98	0.01334	0.10308	7.73		0.02858	0.15057	5.27		0.06679	0.22867	3.42		0.243
		1	1.56	0.02686	0.18869	7.02		0.05804	0.27637	4.76		0.13875	0.42248	3.04		0.265
		5/3	1.36	0.04517	0.28500	6.31		0.09880	0.41831	4.23		0.24531	0.64244	2.62		0.292
		3	1.21	0.08291	0.44009	5.31		0.18641	0.64715	3.47		0.52540	0.99797	1.90		0.341
round bar	tension	1/30	4.78	0.00087	0.00752	8.64		0.00184	0.01093	5.94		0.00422	0.01640	3.89		0.222
		1/15	3.47	0.00171	0.01481	8.66		0.00363	0.02152	5.94		0.00828	0.03227	3.90		0.225
		1/9	2.77	0.00278	0.02418	8.70		0.00590	0.03514	5.96		0.01344	0.05271	3.92		0.230
		1/5	2.18	0.00480	0.04189	8.73		0.01016	0.06086	5.99		0.02303	0.09129	3.96		0.239
		1/3	1.81	0.00752	0.06623	8.81		0.01589	0.09622	6.06		0.03577	0.14434	4.04		0.252
		1/2	1.59	0.01050	0.09366	8.92		0.02212	0.13608	6.15		0.04943	0.20412	4.13		0.267
		1	1.33	0.01739	0.1622	9.33		0.03634	0.23570	6.49		0.07978	0.35355	4.43		0.308
		5/3	1.21	0.02356	0.23415	9.94		0.04888	0.34021	6.96		0.10550	0.51031	4.84		0.356
		3	1.12	0.03083	0.3441	11.16		0.06337	0.5000	7.89		0.13401	0.7500	5.60		0.436
round bar	tension	1/30	5.65	0.000374	0.00745	8.52		0.00186	0.01081	5.81		0.00426	0.01620	3.80		0.224
		1/15	4.05	0.00175	0.01467	8.38		0.00373	0.02131	5.72		0.00855	0.03192	3.73		0.227
		1/9	3.18	0.00293	0.02404	8.22		0.00623	0.03491	5.60		0.01434	0.05232	3.65		0.231
		1/5	2.45	0.00532	0.04192	7.88		0.01134	0.06090	5.37		0.02619	0.09136	3.49		0.239
		1/3	1.98	0.00898	0.06686	7.44		0.01922	0.09719	5.06		0.04467	0.14591	3.27		0.249
		3/5	1.61	0.01655	0.11103	6.71		0.03560	0.16143	4.53		0.08389	0.24250	2.89		0.270
		1	1.39	0.02830	0.16646	5.88		0.06138	0.24199	3.94		0.14797	0.36352	2.46		0.300
		5/3	1.25	0.04862	0.24036	4.94		0.10693	0.34940	3.27		0.26999	0.52462	1.94		0.347

# APPENDIX D: STRESS DISTRIBUTIONS AROUND ELLIPTICAL HOLES IN AN INFINITE SHEET

Equations presented below were derived from the general solution presented in a textbook by Timoshenko and Goodier [18]. The solution in that book was based on the work of Stevenson.

Elliptical hole with  $\beta = 90^\circ$



The stress at infinity (S) is under an angle  $\beta = 90^\circ$  with the X-axis. Elliptical co-ordinates are related to the Cartesian co-ordinates by:

$$x = c \cosh \xi \cos \eta \quad (D1a)$$

$$y = c \sinh \xi \sin \eta \quad (D1b)$$

For the semi-axes:

$$a = c \cosh \xi_0, \quad b = c \sinh \xi_0 \quad (D2)$$

The relations for the stress components are (in case of  $\pm$  or  $\mp$  read top sign):

$$\begin{aligned} \frac{\sigma_x + \sigma_y}{S} &= \frac{(1 \pm e^{2\xi_0}) \sinh 2\xi}{\cosh 2\xi - \cos 2\eta} \mp e^{2\xi_0} \\ \frac{\sigma_y - \sigma_x}{S} &= \frac{(1 \pm e^{2\xi_0})}{(\cosh 2\xi - \cos 2\eta)^3} \left[ -\cosh \xi \cos \eta (\sinh 3\xi \cos 3\eta - \right. \\ &\quad \left. - 3 \sinh \xi \cos \eta) - \right. \\ &\quad \left. - \sinh \xi \sin \eta (-\cosh 3\xi \sin 3\eta + 3 \cosh \xi \sin \eta) \right. \\ &\quad \left. + \frac{1}{2} \cosh 2\xi_0 \{ \sinh 4\xi \cos 2\eta - \sinh 2\xi (3 - \cos 4\eta) \} \right] \\ &\quad \pm e^{2\xi_0} \cosh 2\xi_0 \left[ 1 - \tanh 2\xi_0 \frac{\sinh 2\xi}{(\cosh 2\xi - \cos 2\eta)} \right] \quad (D4) \end{aligned}$$

$$\begin{aligned} \frac{2\tau_{xy}}{S} &= \frac{1 \pm e^{2\xi_0}}{(\cosh 2\xi - \cos 2\eta)^3} \left[ \sinh \xi \sin \eta (\sinh 3\xi \cos 3\eta - \right. \\ &\quad \left. - 3 \sinh \xi \cos \eta) - \right. \\ &\quad \left. - \cosh \xi \cos \eta (-\cosh 3\xi \sin 3\eta + 3 \cosh \xi \sin \eta) \right. \\ &\quad \left. + \frac{1}{2} \cosh 2\xi_0 \{ \sin 2\eta (3 - \cosh 4\xi) - \sin 4\eta \cosh 2\xi \} \right] \\ &\quad \pm e^{2\xi_0} \sinh 2\xi_0 \frac{\sin 2\eta}{(\cosh 2\xi - \cos 2\eta)} \quad (D5) \end{aligned}$$

From these equations the maximum principal stress is obtained from the wellknown formula:

$$s_1 = \frac{\sigma_x + \sigma_y}{2} + \left[ \left( \frac{\sigma_y - \sigma_x}{2} \right)^2 + \tau_{xy}^2 \right]^{1/2} \quad (D6)$$



Along the X-axis ( $\eta = 0, y = 0$ )  $\tau_{xy} = 0$  and thus  $S_1 = \sigma_y$ , which is obtained by summing Equations (D3) and (D4). Substitution of  $\eta = 0$  and replacing the  $\xi_0$  function by a/b functions obtained from Eq. (D2) lead to:

$$\frac{(\sigma_y)_{y=0}}{S} = \frac{\left(\frac{a}{b} + 1\right) + \frac{a}{b} \coth \xi \left[\left(\frac{a}{b}\right)^2 - \frac{a}{b} - 3 + \coth^2 \xi\right]}{\left(\frac{a}{b} + 1\right) \left(\frac{a}{b} - 1\right)^2} \quad (D7)$$

Defining:

$$\gamma = \frac{(\sigma_y)_{y=0}}{\sigma_{\text{peak}}} \quad (\gamma \leq 1) \quad (D8)$$

$$\gamma = \frac{\left(\frac{a}{b} + 1\right) + \frac{a}{b} \coth \xi \left[\left(\frac{a}{b}\right)^2 - \frac{a}{b} - 3 + \coth^2 \xi\right]}{\left(1 + 2 \frac{a}{b}\right) \left(\frac{a}{b} + 1\right) \left(\frac{a}{b} - 1\right)^2} \quad (D9)$$

For a specific value of  $\gamma$  the corresponding  $\xi$  value has to be obtained from the latter equation by iteration. The distance  $d_1 = x - a$  from the tip of the ellipsis to the point where  $(\sigma_y)_{y=0}$  has dropped to  $\gamma\sigma_{\text{peak}}$  can then be calculated from Eq. (D1a) ( $\eta = 0$ ):

$$\frac{d_1}{a} = \sqrt{1 - \left(\frac{b}{a}\right)^2} \cosh \xi - 1 \quad (D10)$$

Calculated results for  $\gamma = 0.95, 0.90$  and  $0.80$  are presented in table D1.

For the edge of the hole ( $\xi = \xi_0$ ) the stress is:

$$\frac{S_1}{S} = \frac{(\sigma_\eta)_{\xi=\xi_0}}{S} = \frac{(\sinh 2\xi_0 - 1) + e^{2\xi_0} \cos 2\eta}{\cosh 2\xi_0 - \cos 2\eta} \quad (D11)$$

For  $\eta = 0$  ( $x = a, y = 0$ ) this equation leads to the wellknown formula:

$$K_t = \frac{\sigma_{\text{peak}}}{S} = 1 + 2 \frac{a}{b} \quad (\text{D12})$$

The same formula is obtained from Eq. (D9) by substituting  $\xi = \xi_0$  (and  $\coth \xi_0 = a/b$ ).

For  $\eta = \pi/2$  ( $x = 0, y = b$ ) Eq. (D11) leads to  $(\sigma_\eta)_{\xi=\xi_0} = -S$ .  
Defining:

$$\gamma = \frac{(\sigma_\eta)_{\xi=\xi_0}}{\sigma_{\text{peak}}} \quad (\gamma \leq 1) \quad (\text{D13})$$

the value of  $\eta$  where a specific value of  $\gamma$  applies is found from:

$$\cos 2\eta = \frac{\gamma \left(1 + 2 \frac{a}{b}\right) \left(\frac{a^2}{b^2} + 1\right) - \left(1 + 2 \frac{a}{b} - \frac{a^2}{b^2}\right)}{\gamma \left(1 + 2 \frac{a}{b}\right) \left(\frac{a^2}{b^2} - 1\right) + \left(1 + \frac{a}{b}\right)^2} \quad (\text{D14})$$

The y-co-ordinate  $d_2$  where  $(\sigma_\eta)_{\xi=\xi_0}$  has dropped to  $\gamma\sigma_{\text{peak}}$  is then calculated from Eqs. (D1b) and (D2):

$$\frac{d_2}{a} = \frac{b}{a} \sin \eta \quad (\text{D15})$$

Calculated results are presented in Table D1.

Finally the gradient coefficient defined by:

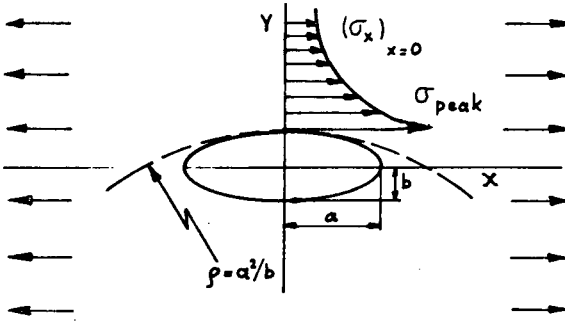
$$\left(\frac{d\sigma}{dx}\right)_{x=a} = -\alpha \frac{\sigma_{\text{peak}}}{\rho} = -\alpha \frac{K_t S}{\rho} \quad (\text{D16})$$

is easily obtained by differentiation of Eq. (D7), subsequent substitution

of  $\xi = \xi_0$  and adopting Eq. (D2), where  $(d\xi/dx)_{\xi=\xi_0} = 1/a$  follows from Eq. (D1a) ( $\eta = 0$ ). The surprisingly simple result obtained is:

$$\alpha = \frac{3 + 4 \frac{a}{b}}{1 + 2 \frac{a}{b}} = 2 + \frac{1}{K_t} \quad (D17)$$

Elliptical hole with  $\beta = 0^\circ$



Equations (D3), (D4) and (D5) apply also here, but now the bottom sign has to be used, wherever  $\pm$  or  $\mp$  occurs.

Along the Y-axis ( $\eta = \pi/2$ ,  $x = 0$ )  $\tau_{xy} = 0$  and thus  $S_1 = \sigma_x$ , which is obtained by subtracting Eqs. (D3) and (D4). Substitution of  $\eta = 0$  and replacing the  $\xi_0$  functions by  $a/b$  functions to be obtained from Eq. (D2) lead to:

$$\frac{(\sigma_x)_{x=0}}{S} = \frac{\left(\frac{b}{a} + 1\right) + \frac{b}{a} \operatorname{tgh} \xi \left[ \left(\frac{b}{a}\right)^2 - \frac{b}{a} - 3 + \operatorname{tgh}^2 \xi \right]}{\left(\frac{b}{a} + 1\right) \left(1 - \frac{b}{a}\right)^2} \quad (D18)$$

With  $\gamma$  now defined as:

$$\gamma = \frac{(\sigma_x)_{x=0}}{\sigma_{\text{peak}}} \quad (\gamma \leq 1) \quad (D19)$$

$$\gamma = \frac{\left(\frac{b}{a} + 1\right) + \frac{b}{a} \operatorname{tgh} \xi \left[ \left(\frac{b}{a}\right)^2 - \frac{b}{a} - 3 + \operatorname{tgh}^2 \xi \right]}{\left(1 + 2 \frac{b}{a}\right) \left(\frac{b}{a} + 1\right) \left(1 - \frac{b}{a}\right)^2} \quad (D20)$$

Again the value of  $\xi$  for a specific  $\gamma$  value has to be obtained by iteration. The distance  $d_1 = y - b$  from the point of maximum stress ( $y = b, x = 0$ ) to the point where  $(\sigma_x)_{x=0}$  has dropped to  $\gamma \sigma_{\text{peak}}$  can be calculated from Eq. (D1b) ( $\eta = \pi/2$ ):

$$\frac{d_1}{b} = \sqrt{\left(\frac{a}{b}\right)^2 - 1} \sinh \xi - 1 \quad (\text{D21})$$

Calculated results are presented in table D1.

For the stress at the edge of the hole the result is:

$$\frac{S_1}{S} = \frac{(\sigma_\eta)_{\xi=\xi_0}}{S} = \frac{(\sinh 2\xi_0 + 1) - e^{2\xi_0} \cos 2\eta}{\cosh 2\xi_0 - \cos 2\eta} \quad (\text{D22})$$

The peak stress now occurs at  $\eta = \pi/2$  ( $x = 0, y = b$ ) which gives:

$$K_t = \frac{\sigma_{\text{peak}}}{S} = 1 + 2 \frac{b}{a} \quad (\text{D23})$$

For  $\eta = 0$  ( $x = a, y = 0$ ) again  $\sigma_\eta = -S$  is found.

Defining again  $\gamma$  as it has been done before (Eq. D13) the relation obtained is:

$$\cos 2\eta = \frac{\gamma \left(1 + 2 \frac{b}{a}\right) \left(\frac{a^2}{b^2} + 1\right) + \left(1 - 2 \frac{a}{b} - \frac{a^2}{b^2}\right)}{\gamma \left(1 + 2 \frac{b}{a}\right) \left(\frac{a^2}{b^2} - 1\right) - \left(1 + \frac{a}{b}\right)^2} \quad (\text{D24})$$

The x-co-ordinate  $d_2$  where  $(\sigma_\eta)_{\xi=\xi_0}$  has dropped to  $\gamma \sigma_{\text{peak}}$  is then calculated from Eqs. (D1a) and (D2):

$$\frac{d_2}{b} = \frac{a}{b} \cos \eta \quad (\text{D25})$$

Calculated results are presented in table D1.

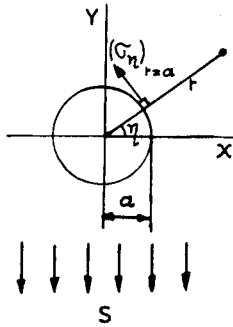
Differentiation of Eq. (D18) leads to a similar formula for the stress gradient coefficient as presented before (Eq. D17). The result is:

$$\alpha = \frac{3 + 4 \frac{b}{a}}{1 + 2 \frac{b}{a}} = 2 + \frac{1}{K_t} \quad (D17a)$$

### Circular hole

With elliptical co-ordinates a circular hole is obtained if  $\xi_0 \rightarrow \infty$ . All other ellipses  $\xi = \text{constant}$  ( $\xi > \xi_0$ ) also become circles and the hyperboles ( $\eta = \text{constant}$ ) become straight lines:

$$y = x \operatorname{tg} \eta \quad (D26)$$



With  $r$  and  $\eta$  as polar co-ordinates the equations for the three stress components are:

$$\frac{\sigma_x + \sigma_y}{S} = 1 + 2 \left( \frac{a}{r} \right)^2 \cos 2\eta \quad (D27)$$

$$\frac{\sigma_y - \sigma_x}{S} = 1 + \left( \frac{a}{r} \right)^2 (\cos 2\eta - 2 \cos 4\eta) + 3 \left( \frac{a}{r} \right)^4 \cos 4\eta \quad (D28)$$

$$\frac{2\tau_{xy}}{S} = \left( \frac{a}{r} \right)^2 (2 \sin 4\eta - \sin 2\eta) - 3 \left( \frac{a}{r} \right)^4 \sin 4\eta \quad (D29)$$

Along the X-axis ( $y = 0$ ,  $\eta = 0$ )  $\tau_{xy} = 0$  and  $S_1 = \sigma_y$ . From Eqs. (D27) and (D28):

$$\frac{S_1}{S} = \frac{(\sigma_y)_{y=0}}{S} = 1 + \frac{1}{2} \left(\frac{a}{r}\right)^2 + \frac{1}{2} \left(\frac{a}{r}\right)^4 \quad (D30)$$

For  $r = a$  the wellknown  $K_t = 3$  is obtained.

The value of  $r$  where  $(\sigma_y)_{y=0}$  has dropped to  $\gamma \sigma_{\text{peak}}$  is easily deduced from equation (D30):

$$\frac{r}{a} = \left[ \frac{-1 + \sqrt{1 + 12(6\gamma - 2)}}{6} \right]^{-\frac{1}{2}} \quad (D31)$$

The corresponding distance from the edge of the hole is  $d_1 = r - a$ . Calculated results are given in table D1.

Along the edge of the hole ( $r = a$ )  $S_1 = (\sigma_\eta)_{r=a} = \sigma_x + \sigma_y$ . From Eq. (D27):

$$\frac{S_1}{S} = \frac{(\sigma_\eta)_{r=a}}{S} = 1 + 2 \cos 2\eta \quad (D32)$$

The location where  $(\sigma_\eta)_{r=a}$  has dropped to  $\gamma \sigma_{\text{peak}}$  is given by

$$\eta = \frac{1}{2} \text{bg} \cos \left( \frac{3\gamma - 1}{2} \right) \quad (D33)$$

The corresponding y-co-ordinate  $d_2 = a \sin \eta$ .

#### Calculated results

Values of  $d_1$  and  $d_2$  have been calculated for a drop of the stress from the peak value at the root of the notch ( $\sigma_{\text{peak}} = K_t S$ ) with an amount of 5%, 10% and 20% respectively, corresponding to  $\gamma = 0.95$ ,  $\gamma = 0.90$  and  $\gamma = 0.80$ . The results are presented in table D1, while  $d_2/d_1$  values are plotted in Figure 6.

The results show that a smaller tip radius ( $\rho$ ) associated with a higher  $K_t$  value gives smaller values of  $d_1$  and  $d_2$ . In other words the stress

both away from the edge (direction of  $d_1$ ) and along the edge of the hole ( $d_2$ ) decays faster for a sharper notch, which should be expected. However, it is surprising that  $d_2/d_1$  hardly varies for large variation of the severity of the stress raiser.

Contours of constant maximum tensile stress (maximum principal stress  $S_1$ ) have been calculated for three holes with  $K_t = 7, 3$  and  $1.67$  respectively. Values of  $S_1$  are obtained from Eq. (D6) by substituting Eqs. (D3) - (D5) for the elliptical holes and Eqs. (D27) - (D29) for the circular hole. The equations then obtained do not allow to calculate explicitly the co-ordinates of the contours for specified values of  $\gamma$ . For the elliptical holes a  $\xi$ -value was adopted and by iteration the  $\eta$ -value was determined to obtain the required  $\gamma$  value. For the circular hole the same procedure was followed for  $\eta$  and  $r/a$  respectively. The calculated points of the contours are presented in the table D2 and in Figures 7a-c. A comparison between the three holes is given in Figure 8 where the scale for each hole was adjusted to obtain equal tip radii ( $\rho$ ). A striking similarity is then obtained for  $\gamma = 1 \rightarrow 0.8$ .

Table D1. Calculated results for elliptical holes

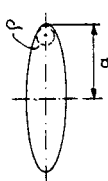
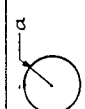
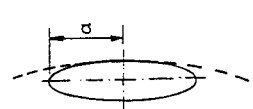
	a/b	$\rho/a$	$K_t$	$\alpha$	$\gamma = 0.95$		$\gamma = 0.90$		$\gamma = 0.80$		$\beta(\gamma=0.95)$ (Eq. 24)
					$d_1/a$	$d_2/a$	$d_1/a$	$d_2/a$	$d_1/a$	$d_2/a$	
	3	0.111	7	2.14	0.00274	0.02371	0.00581	0.03423	0.01324	0.05058	0.234
	2.5	0.16	6	2.17	0.00390	0.03374	0.00827	0.04863	0.01883	0.07160	0.237
	2	0.25	5	2.20	0.00600	0.05185	0.01271	0.07454	0.02891	0.10911	0.241
	1.5	0.444	4	2.25	0.01042	0.08989	0.02207	0.12860	0.05014	0.18625	0.247
	1	1	3	2.33	0.02258	0.19365	0.04778	0.27386	0.10858	0.38730	0.258
	b/a	$\rho/b$			$d_1/b$	$d_2/b$	$d_1/b$	$d_2/b$	$d_1/b$	$d_2/b$	
	0.6667	2.25	2.33	2.43	0.04877	0.4120	0.1031	0.5708	0.2354	0.7767	0.273
	0.5	4	2	2.50	0.08415	0.6963	0.1782	0.9428	0.4097	1.2344	0.287
	0.3333	9	1.67	2.60	0.1821	1.4230	0.3870	1.8371	0.9136	2.2500	0.316
	0.2	25	1.4	2.71	0.4861	3.2746	1.0484	3.8976	2.7644	4.3805	0.382
	0.1	100	1.2	2.83	1.8997	8.5855	4.4721	9.2319	-	9.6151	0.582



Table D2. Calculated co-ordinates of lines of constant maximum principal stress  $S_1$  for elliptical holes.

$\gamma = S_1/\sigma_{\text{peak}}$   
 (a)  $\rightarrow$  edge of hole

	a/b = 3 $K_t = 7$		a/b = 1 $K_t = 3$		a/b = $\frac{1}{3}$ $K_t = 1\frac{2}{3}$	
	x/a	y/a	x/a	y/a	x/a	y/a
$\gamma = 0.95$	1.0027	0	1.0226	0	0	0.3940
	1.0023	0.0072	1.0212	0.0357	0.1628	0.3823
	1.0016	0.0112	1.0172	0.0711	0.3218	0.3479
	0.9997	0.0183	1.0105	0.1062	0.4209	0.3149
	0.9975(a)	0.0237(a)	1.0012	0.1407	0.4743(a)	0.2934(a)
			0.9892	0.1744		
			0.9811(a)	0.1936(a)		
$\gamma = 0.90$	1.0058	0	1.0478	0	0	0.4623
	1.0054	0.0068	1.0464	0.0365	0.0965	0.4577
	1.0034	0.0167	1.0422	0.0729	0.1631	0.4488
	1.0001	0.0253	1.0353	0.1088	0.2091	0.4400
	0.9969	0.0311	1.0257	0.1442	0.3308	0.4059
	0.9947(a)	0.0342(a)	1.0133	0.1787	0.4137	0.3732
			0.9983	0.2122	0.4792	0.3418
			0.9807	0.2445	0.5344	0.3116
			0.9618(a)	0.2739(a)	0.5827	0.2825
					0.6124(a)	0.2635(a)
$\gamma = 0.80$	1.0132	0	1.1086	0	0	0.6378
	1.0124	0.0106	1.1071	0.0387	0.2102	0.6118
	1.0102	0.0198	1.1027	0.0771	0.3971	0.5395
	1.0033	0.0348	1.0954	0.1151	0.4995	0.4741
	0.9967	0.0432	1.0851	0.1525	0.5713	0.4143
	0.9905	0.0490	1.0719	0.1890	0.6273	0.3591
	0.9884(a)	0.0506	1.0558	0.2244	0.6742	0.3076
			1.0369	0.2585	0.6957	0.2830
			1.0151	0.2911	0.7164	0.2591
			0.9905	0.3218	0.7366	0.2358
			0.9635	0.3507	0.7500	0.2205(a)
			0.9341	0.3774		
			0.9220(a)	0.3873		

Table D2 (Continued)

	a/b = 3 $K_t = 7$		a/b = 1 $K_t = 3$		a/b = $\frac{1}{3}$ $K_t = 1\frac{2}{3}$	
	x/a	y/a	x/a	y/a	x/a	y/a
$\gamma = 0.50$	1.0579	0	1.5175	0	1.2379	0.2842
	1.0564	0.0205	1.5165	0.0530	1.1486	0.2625
	1.0551	0.0275	1.5134	0.1058	1.0758	0.2442
	1.0515	0.0407	1.5083	0.1585	1.0128	0.2322
	1.0472	0.0516	1.5008	0.2109	0.9812	0.2267
	1.0375	0.0676	1.4908	0.2629	0.9515	0.2192
	1.0288	0.0771	1.4781	0.3142	0.9264	0.2073
	1.0209	0.0835	1.4621	0.3646	0.9084	0.1903
	1.0135	0.0880	1.4426	0.4137	0.9024	0.1800
	0.9999	0.0934	1.4189	0.4610	0.8984	0.1687
	0.9876	0.0957	1.3903	0.5060	0.8965	0.1565
	0.9764	0.0961	1.3560	0.5479	0.8964	0.1477(a)
	0.9660	0.0952	1.3150	0.5855		
	0.9611	0.0944	1.2657	0.6173		
	0.9594(a)	0.0940(a)	1.2062	0.6414		
			1.1335	0.6544		
			1.0445	0.6527		
			0.9441	0.6368		
			0.8537	0.6202		
			0.7906(a)	0.6124(a)		

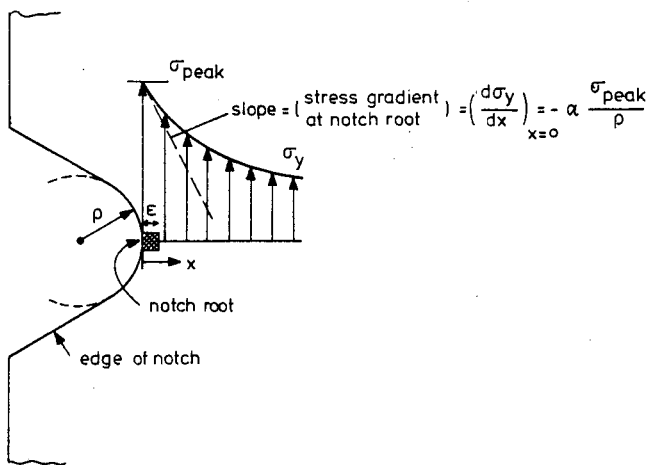


Figure 1: Stress distribution in minimum section

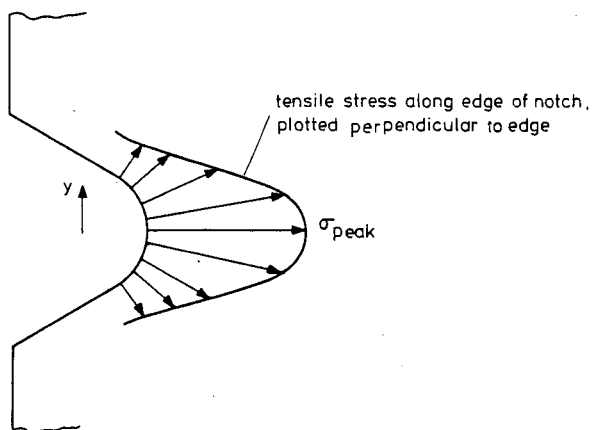


Figure 2: Stress distribution along edge of notch

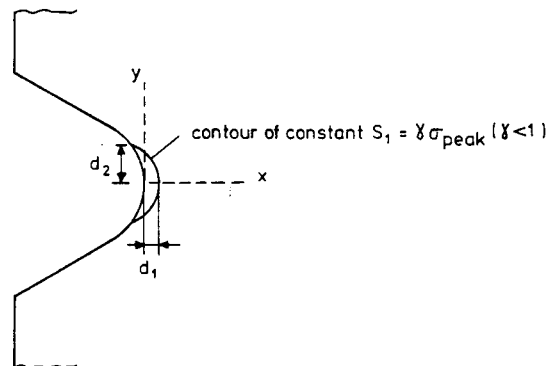
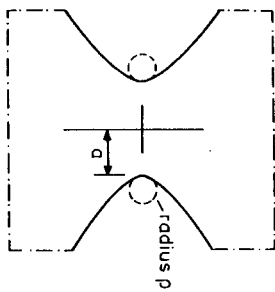
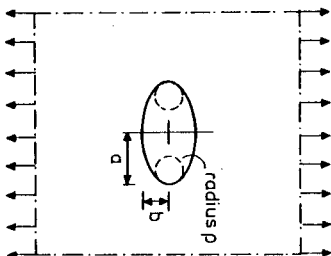


Figure 3: Contour of constant maximum tensile stress

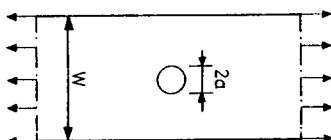
Hyperbolic notches in  
infinite material, flat  
bar or round shaft,  
tension or bending  
(Neuber [21])



Elliptical hole in  
infinite sheet



Strip with  
hole  
(Howland [14])



Row of holes  
(Schulz [15])

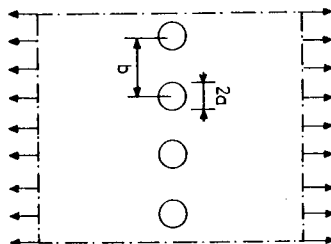


Figure 4: Notches for which  $\alpha$  and  $d/d_1$  have been calculated

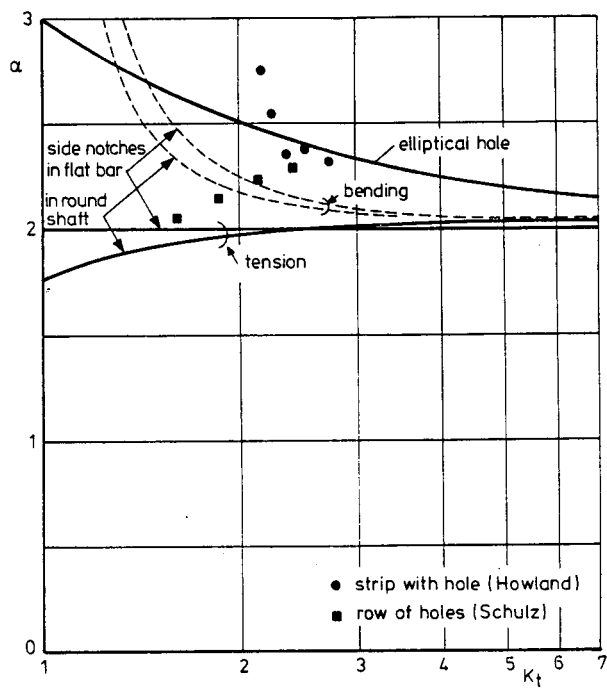


Figure 5: The stress gradient coefficient  $\alpha$  as a function of  $K_t$

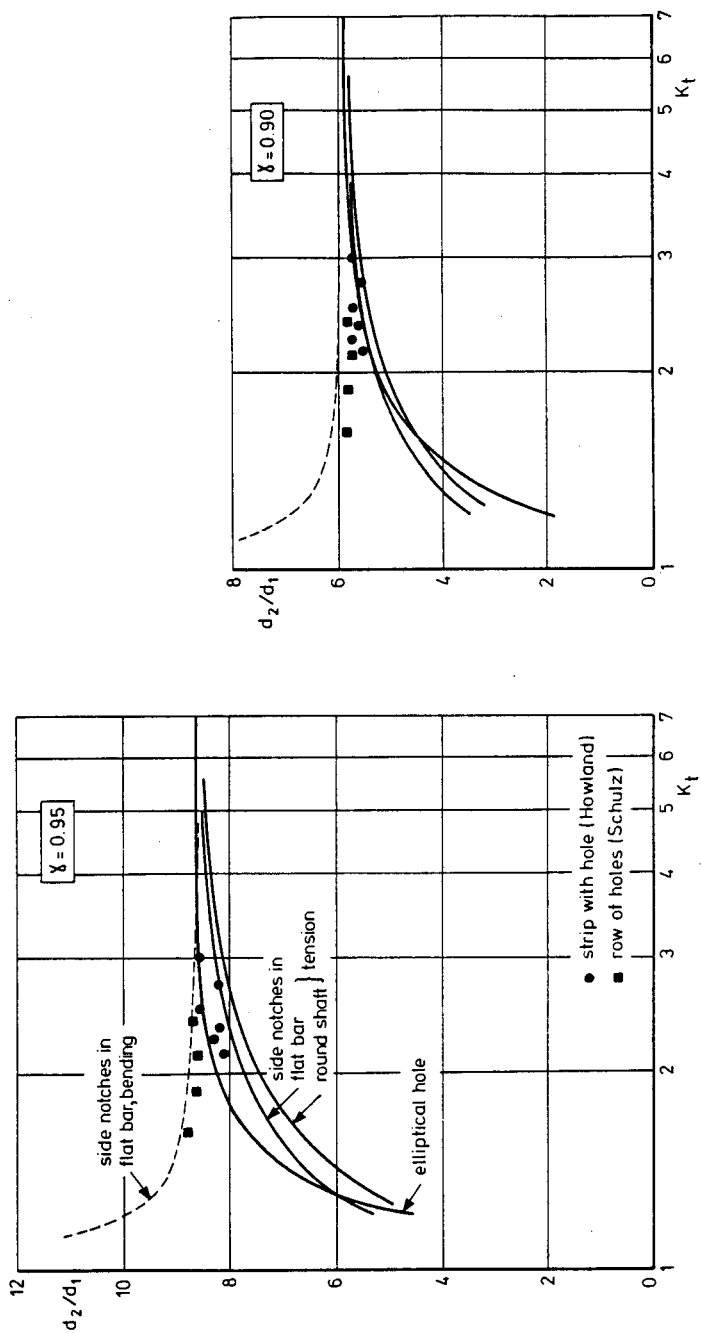
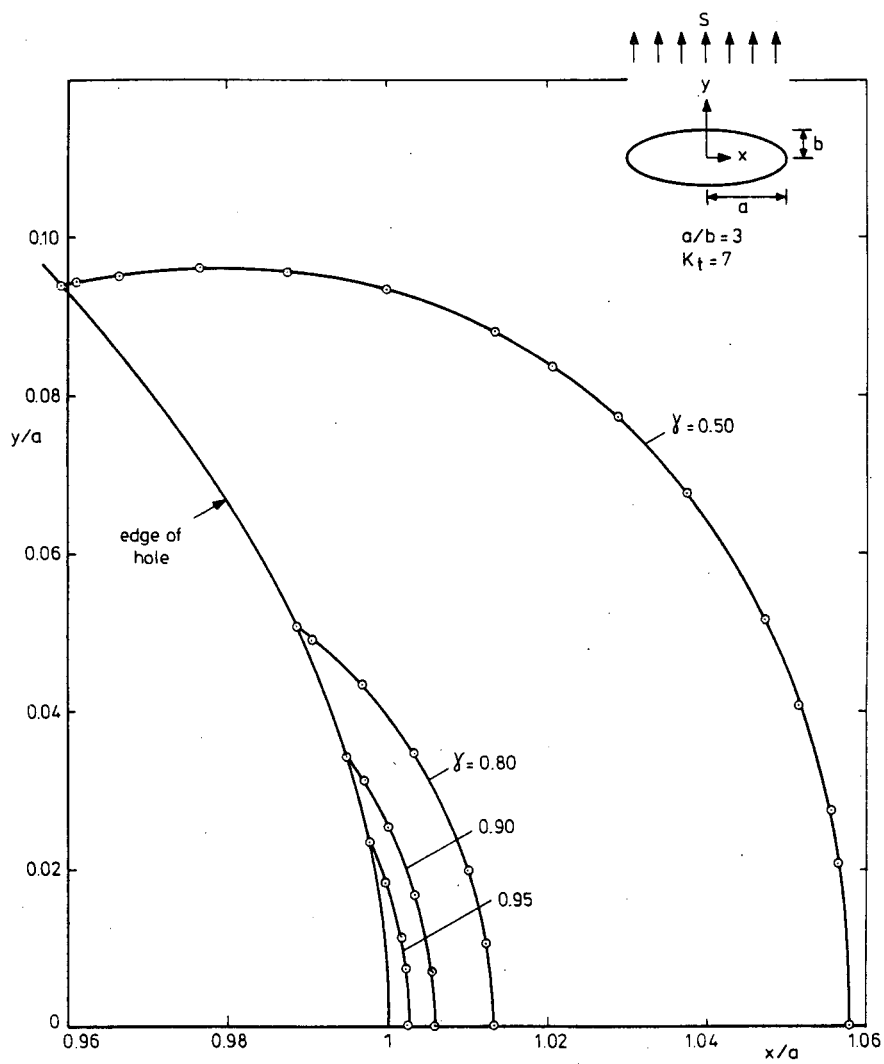


Figure 6: Calculated results for  $d_2/d_1$  as defined in Figure 3

Figure 7a: Lines of constant principal stress ( $\gamma = S_1/\sigma_{\text{peak}}$ )



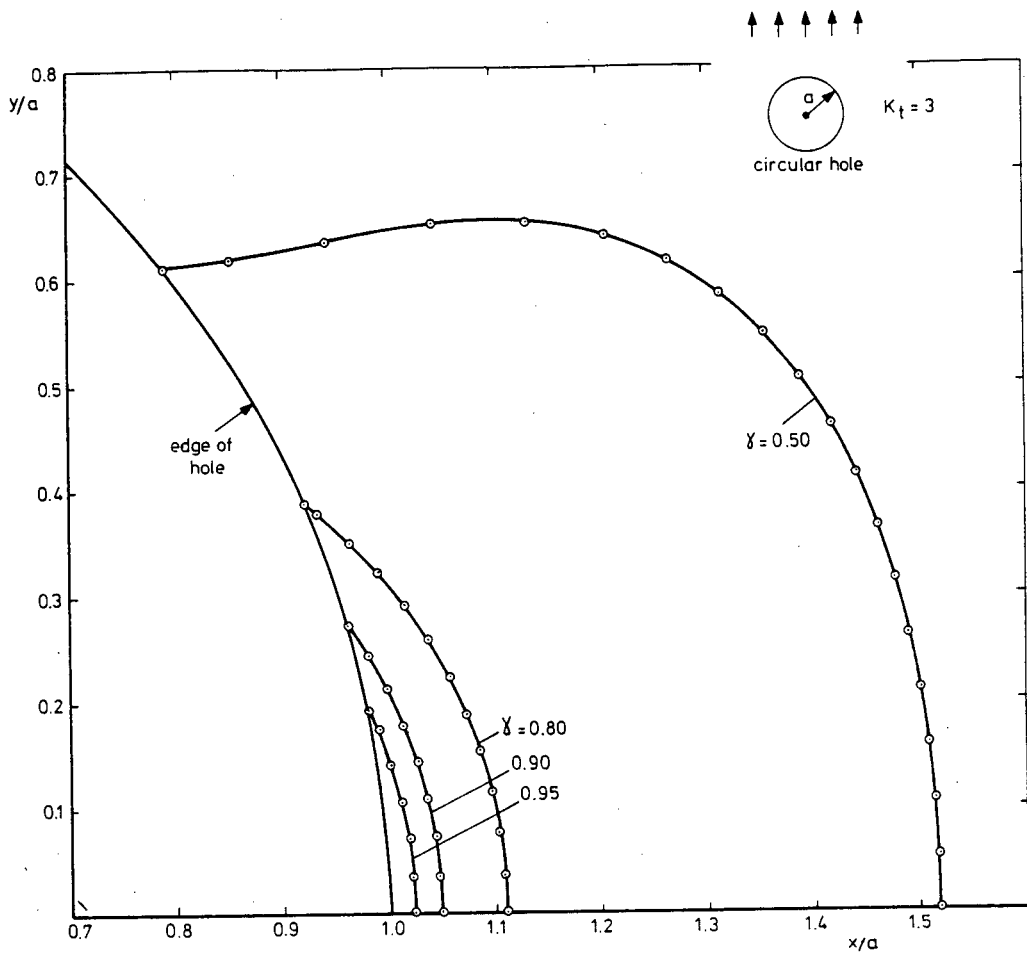


Figure 7b: Lines of constant principal stress ( $\gamma = S_1/\sigma_{\text{peak}}$ )



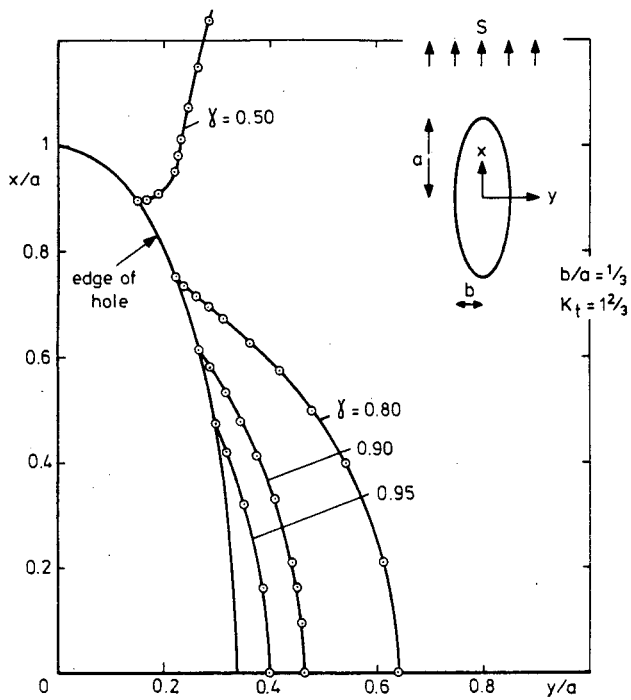


Figure 7c: Lines of constant principal stress ( $\gamma = S_1/\sigma_{\text{peak}}$ )

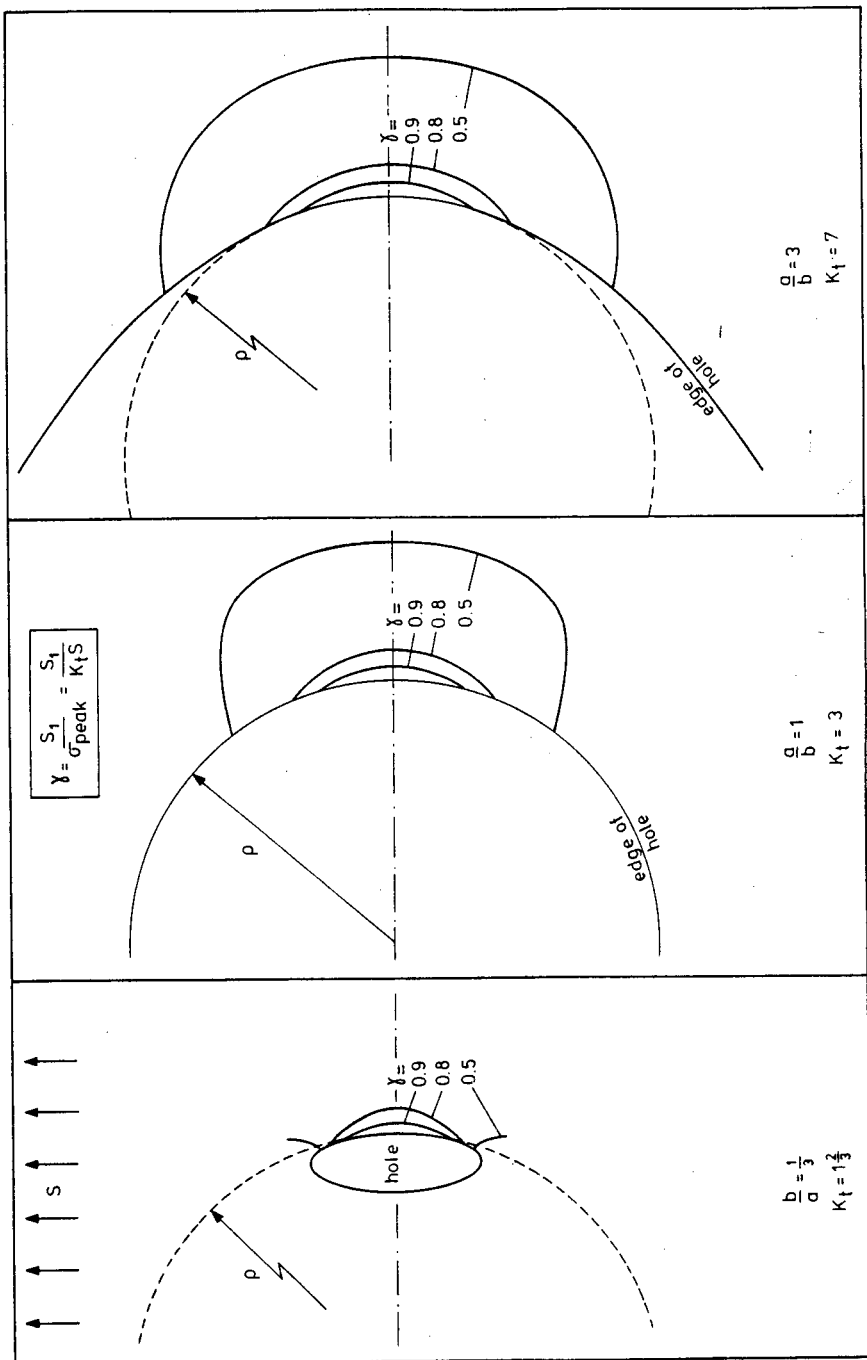


Figure 8: Lines of constant maximum principal stress ( $S_1$ ) around three elliptical holes in an infinite sheet loaded in tension (holes scaled to obtain same  $\rho$ ).

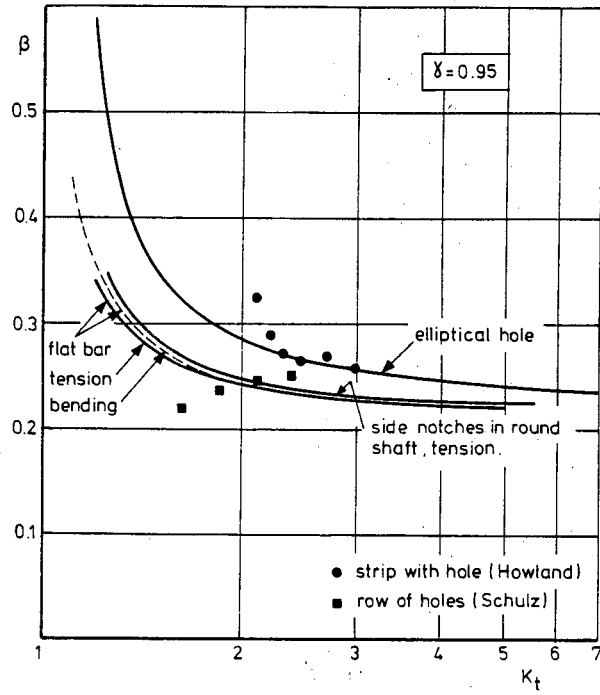


Figure 9: The second stress gradient coefficient  $\beta$  (Eq.23) as a function of  $K_t$

Rapport 297



60141070391